

(Atom) Lasers, Coherent States, and Coherence: an Investigation using Maximally Robust Unravelings

H.M. Wiseman^{1,2*} and John A. Vaccaro²

¹*Department of Physics, University of Queensland, Queensland 4072 Australia.*

²*Division of Physics and Astronomy, University of Hertfordshire, Hatfield AL10 9AB, UK*

A laser, be it an optical laser or an atom laser, is an open quantum system which produces a coherent beam of bosons (photons or atoms respectively). The stationary state of the laser mode is a mixture of coherent field states with random phase, or, equivalently, a Poissonian mixture of number states. This paper attempts to answer the question: which (if either) of these two descriptions is more natural? The approach we use is to find the maximally robust unraveling [H.M. Wiseman and J.A. Vaccaro, Phys. Lett. A **250**, 241 (1998)] of the master equation. The associated ensemble consists of pure states which are robust, that is, which survive relatively unchanged for a long time. In the ideal laser limit, the most robust states are indeed coherent states. As the phase noise is increased, either directly or through self-interaction of the bosons, the most robust states become more and more amplitude-squeezed. We find scaling laws for these states, and give analytical derivations for them. As the phase noise becomes so large that the laser output is no longer quantum coherent, the most robust states cease to have a well-defined coherent amplitude. Thus quantum coherence of the laser output is manifest in the most natural description of the state of the laser mode being in terms of states with a well-defined coherent amplitude. This justifies our approach based on maximally robust unravelings, and also has interesting implications for atom lasers in particular, for which phase noise due to self-interactions is expected to be large.

03.65.Bz, 03.75.Fi, 42.50.Lc, 05.30.-d

I. INTRODUCTION

In elementary presentations of quantum optics it is more or less an axiom that lasers produce coherent light. In semiclassical presentations this means that the field is represented by a *c*-number α , while in a fully quantum treatment it is represented by a coherent state $|\alpha\rangle$.

Recently, it has been argued that both of these representations are fictions, albeit convenient ones [1]. The essential argument is that no commonly employed process at optical frequencies produces an electric field having a non-zero average amplitude. While this point of view is certainly defensible [2], it perhaps obscures the fact that there is something special about laser light.

In Ref. [3], one of us argued that what is special about laser light is that it is well approximated by a noiseless classical electromagnetic wave. Four quantitative criteria were given, none of which require a mean field, so there is no dispute with Ref. [1]. The least familiar, and so most important, of these criteria is that the output flux of the laser (bosons per unit time) must be much greater than its spectral linewidth. Put another way, the coherence time of a true laser must be much greater than the mean temporal separation of photons in the output beam. This is typically satisfied by many orders of magnitude in optical lasers, but is not satisfied by ordinary thermal sources.

This concept of quantum coherence is quite distinct from the elementary idea that a laser is in a coherent state. Indeed, theoretical models for typical laser processes imply that the state of the cavity mode for a laser far above threshold is a mixture of coherent states of all phases. That is to say, the stationary state matrix of the laser mode can be written

$$\rho_{ss} = \int \frac{d\phi}{2\pi} \left| |\alpha| e^{i\phi} \right\rangle \left\langle \left| |\alpha| e^{i\phi} \right| \right|, \quad (1.1)$$

where $|\alpha|^2 = \mu$ is the mean number of photons in the laser.

It would be tempting to interpret Eq. (1.1) to mean that the laser really is in a coherent state $|\alpha| e^{i\phi}$ of definite phase ϕ , but we don't know what that phase is. However, this temptation must be resisted because the stationary state matrix can also be written

$$\rho_{ss} = \sum_{n=0}^{\infty} e^{-\mu} \frac{\mu^n}{n!} |n\rangle \langle n|, \quad (1.2)$$

which would seem to imply that the laser really is in a number state $|n\rangle$, but we don't know which number it is.

Given that the unknown coherent state description and the unknown number state description are mathematically equivalent, why is the former ubiquitous and the latter rare? The answer, as was pointed out some time ago by Gea-Banacloche [4], is differential survival times.

*Electronic address: wiseman@physics.uq.edu.au

A laser prepared in a coherent state will remain close to that initial state for a time of order κ^{-1} , where κ is the bare decay rate of the cavity. By contrast, a laser prepared in a number state will be likely to remain in that state only for a time of order κ^{-1}/μ , where μ is the mean number as above.

This result, derived also in Ref. [5], was taken further by Gea-Banacloche in Ref. [6] using the early model for a laser with saturation due to Scully and Lamb [7]. Gea-Banacloche considered pure states with mean photon equal to that of the laser at steady state, and calculated their purity at later times. He showed that the pure state which had the slowest initial rate of decay of purity was in general a slightly amplitude-squeezed state rather than a coherent state.

A calculation for a Bose-Einstein condensate by one of us with Barnett and Burnett [8] produced similar results. In this case the analysis was based on the fidelity [9] which measures the overlap of the initial state with the state at a later time.

There seems little doubt, then, that it is most useful to consider an ideal laser to be in a coherent state (or nearly coherent state) of unknown phase. However it is an open question whether this is true of a non-ideal laser, that is, a laser with additional noise of some form. Another open question is how this issue relates to the quantum coherence of the output of such a non-ideal device.

A particular system of interest is the atom laser. This is a device which would produce an output beam of bosonic atoms analogous to an optical laser's beam of photons [3]. The idea for an atom laser was published independently by a number of authors [10–13], shortly after the first achievement of Bose-Einstein condensation of weakly interacting atoms [14–16]. There have since been some important advances in the coherent release of pulses [17,18] and beams [19,20] of atoms from a condensate. Because the condensate is not replenished in these experiments, the output coupling cannot continue indefinitely, so these devices cannot be considered true lasers. Nevertheless they represent the first steps towards achieving a continuously operating atom laser.

An important difference between an atom laser and an optical laser is that the interatomic interactions cannot be neglected. The atoms may be weakly interacting in the sense of forming a gas rather than a liquid, but still the elastic collisions may dominate the dynamics of the condensate.

The analysis in Ref. [8] did use a model for a condensate which included self-interactions. However, Ref. [8] only calculated the initial rate of decay of the fidelity, and this is unaffected by any Hamiltonian terms. Hence the self energy played no role in this analysis. Moreover, the treatment, like that of Gea-Banacloche [6], considered only a single pure state to represent the state of the condensate. Thus it does not give, in general, a representation of the steady state on par with Eq. (1.1) or Eq. (1.2).

In this paper we give an analysis of the dynamics at all

times and which incorporates an ensemble of pure states. It takes into account Hamiltonian terms and gives a robust representation of the steady state. We find that the self-interactions have an important influence on the robustness of the pure states.

The analysis we use is that of finding the “maximally robust unraveling” (MRU) for the system's master equation. This technique was recently proposed by us as a general tool for open quantum systems [21]. In Sec. II we recapitulate our proposal, and compare it to other approaches. In Sec. III we present our atom laser model, including self-interactions and phase diffusion. In Sec. IV we explain how to find the MRU for this model and in Sec. V present the results of this search. Sec. VI concludes with a discussion of our results, their relationship to the quantum coherence of the atom laser output, and their implications for the current state of experimental atom lasers.

II. MAXIMALLY ROBUST UNRAVELINGS

A. Comparison with Other Approaches

The idea of robustness has its origins in studies of decoherence and the classical limit [4–6,8,22–25]. Decoherence is the process by which an open quantum system becomes entangled with its environment, thereby causing its state to become mixed. However, not all pure states decohere with equal rapidity. In particular, Zurek [22] defined the “preferred states” of open quantum systems as those states which remain relatively pure for a long time.

This idea can be thought of as a “predictability sieve” [23]. That is, the preferred states are those for which the future dynamics are predictable, in the sense that there is some projective question (is the system in some particular state?) which is likely to give the result “yes”.

Our approach of defining the maximally robust unraveling [21] shares some similarities with these earlier approaches. There are, however, a number of key differences.

1. Ensembles of Pure States

First, we consider not a single pure state, but an ensemble of pure states. This is appropriate for situations where the open system comes to a mixed equilibrium state. The ensemble of pure states which we consider must be a representation of that equilibrium mixed state. That is, the system has a certain probability of being in one of those pure states, as in Eqs. (1.1) and (1.2).

Without considering such an ensemble it is necessary to put some ad-hoc restriction on the pure states considered so that they have some relevance to actual state the system is in at equilibrium. For example, as noted above,

Gea-Banacloche [6] considered only pure states having the same mean photon number as the equilibrium state of the laser model under consideration.

2. Physical Realizability

Second, we place a restriction on the ensembles of pure states which we consider: they must be physically realizable. By this we mean that it should be possible, without altering the evolution of the system, to know that its state at equilibrium is definitely one of the pure states in the ensemble, but *which* pure state cannot be predicted beforehand.

It may seem contradictory to say that the system at equilibrium is mixed, but that nevertheless we can know it to be in a pure state. The resolution is that, by monitoring the system's environment, the system state can, under suitable circumstances, be collapsed over time into a pure state. Being simply an example of a quantum measurement, this process, called an *unraveling* [26], will be stochastic. *On average*, the system evolution is not changed and the ensemble of pure states produced by the unraveling is guaranteed to be equivalent to the equilibrium mixed state.

3. Survival Probability

Third, we define robustness in terms of the survival probability of the pure states rather than their purity. That is, we consider how close the states remain to their original state, not simply how close they remain to a pure state. This means that Hamiltonian evolution alone can affect the robustness of states (whereas it doesn't affect their purity, except in conjunction with the irreversible terms). It might be thought that this is an undesirable feature. The reasons behind our choice will be elaborated later. However the best justification is that, as will be shown, using the survival probability gives results which accord with intuition, whereas using purity does not.

4. Survival Time

The final aspect of our work which differs from most previous approaches [6,24,25] is that we quantify the robustness by the survival time. This is the time taken for the survival probability to fall below some predefined threshold. This is as opposed to considering the rate of decay of the survival probability at the initial time. That rate is actually identical to half the initial rate of decay of the purity, and hence is independent of any Hamiltonian terms. It is only by considering the robustness over some finite time that the Hamiltonian terms will contribute.

B. Unraveling the Master Equation

1. The Master Equation

Open quantum systems generally become entangled with their environment, and this causes their state to become mixed. In many cases, the system will reach an equilibrium mixed state in the long time limit. This is the sort of system for which our approach to robustness, of finding the maximally robust unraveling (MRU), can be applied without modification.

If the system is weakly coupled to the environmental reservoir, and many modes of the reservoir are roughly equally affected by the system, then one can make the Born and Markov approximations in describing the effect of the environment on the system [27]. Tracing over (that is, ignoring) the state of the environment leads to a Markovian evolution equation for the state matrix ρ of the system, known as a *quantum master equation*. The most general form of the quantum master equation which is mathematically valid is the Lindblad form [28]

$$\dot{\rho} = -i[H, \rho] + \sum_{k=1}^K \mathcal{D}[c_k] \rho \equiv \mathcal{L}\rho, \quad (2.1)$$

where for arbitrary operators A and B ,

$$\mathcal{D}[A]B \equiv ABA^\dagger - \{A^\dagger A, B\}/2. \quad (2.2)$$

If the master equation has a unique stationary state (as we will assume it does), then that is defined by

$$\mathcal{L}\rho_{ss} = 0 \quad (2.3)$$

This assumption requires that \mathcal{L} be time-independent. In many quantum optical situations, one is only interested in the dynamics in the interaction picture, in which the free evolution at optical frequencies is removed from the state matrix. Indeed, for quantum systems driven by a classical field, it may be necessary to move into such an interaction picture in order to obtain a time-independent Liouvillian superoperator \mathcal{L} .

The stationary state matrix ρ_{ss} can be expressed as an ensemble of pure states as follows:

$$\rho_{ss} = \sum_i w_i P_i, \quad (2.4)$$

where the P_i are projection operators

$$P_i^2 = P_i, \quad (2.5)$$

and the w_i are positive weights summing to unity. The (possibly infinite) set of ordered pairs,

$$E = \{P_i, w_i\}_i, \quad (2.6)$$

we will call an ensemble E of pure states. Note that there is no restriction that the projectors P_i be mutually orthogonal. This means that there are continuously infinitely many ensembles E which represent ρ_{ss} . The aim of finding the MRU is to find the “most natural” representation for ρ_{ss} .

2. Unravelings

As explained in Sec. II A 2 above, the first criterion for our most natural ensemble is that it be physically realizable by monitoring the environment of the system. In the situation where a Markovian master equation can be derived, it is possible (in principle) to continually measure the state of the environment on a time scale large compared to the reservoir correlation time but small compared to the response time of the system. This effectively continuous measurement is what we mean by “monitoring”. In such systems, monitoring the environment does not disrupt the system–reservoir coupling and the system will continue to evolve according to the master equation if one ignores the results of the monitoring.

By contrast, if one does take note of the results of monitoring the environment, then the system will no longer obey the master equation. Because the system–reservoir coupling causes the reservoir to become entangled with the system, measuring the former’s state produces information about the latter’s state. This will tend to undo the increase in the mixedness of the system’s state caused by the coupling.

If one is able to make perfect rank-one projective (i.e. von Neumann) measurements of the reservoir state, the system state will usually be collapsed towards a pure state. However this is not a process which itself can be described by projective measurements on the system, because the system is not being directly measured. Rather, the monitoring of the environment leads to a gradual (on average) decrease in the system’s entropy.

If the system is initially in a pure state then, under perfect monitoring of its environment, it will remain in a pure state. Then the effect of the monitoring is to cause the system to change its pure state in a stochastic and (in general) nonlinear way. Such evolution has been called a quantum trajectory [26], and can be described by a nonlinear stochastic Schrödinger equation [29–31]. The nonlinearity and stochasticity are present because they are a fundamental part of measurement in quantum mechanics.

Although a stochastic Schrödinger equation is conceptually the simplest way to define a quantum trajectory, in this work we will instead use the stochastic master equation (SME) [31]. This has two advantages. First, it is more general in that it can describe the purification of an initially mixed state. Second, it is easier to see the relation between the quantum trajectories and the master equation which the system still obeys on average.

Assuming that the initial state of the system is pure, the quantum trajectory for its projector will be described by the SME

$$dP = dt (\mathcal{L} + \mathcal{U}) P. \quad (2.7)$$

Here \mathcal{L} is the Liouvillian superoperator from the master equation, and \mathcal{U} is a stochastic superoperator which is, in general, nonlinear in its operation on P . It also depends on the operators c_k as defined in Eq. (2.1), and is constrained by the following two equations which must hold for arbitrary projectors P

$$\{P, (\mathcal{L} + \mathcal{U})P\} + dt[\mathcal{U}P][\mathcal{U}P] = (\mathcal{L} + \mathcal{U})P, \quad (2.8)$$

$$\mathbb{E}[\mathcal{U}P] = 0. \quad (2.9)$$

The first of these properties ensures that $P + dP$ is a projector if P is a projector; that is, that the state remains pure. The second ensures that

$$d\mathbb{E}[P] = \mathcal{L}\mathbb{E}[P]dt, \quad (2.10)$$

where \mathbb{E} denotes the ensemble-averaged with respect to the stochasticity of \mathcal{U} . This stochasticity is evidenced by the necessity of retaining the term $dt[\mathcal{U}P][\mathcal{U}P]$ in Eq. (2.8).

Because the ensemble average of the system still obeys the master equation, the stochastic master equation (or equivalently the stochastic Schrödinger equation) is said to *unravel* the master equation [26]. It is now well-known that there are many (in fact continuously many) different unravelings for a given master equation [32], corresponding to different ways of monitoring the environment.

For simplicity we will call \mathcal{U} an unraveling. Each unraveling gives rise to an ensemble of pure states

$$E^{\mathcal{U}} = \{P_i^{\mathcal{U}}, w_i^{\mathcal{U}}\}_i, \quad (2.11)$$

where $P_i^{\mathcal{U}}$ are the possible pure states of the system at steady state, and $w_i^{\mathcal{U}}$ are their weights. For master equations with a unique stationary state ρ_{ss} , the SME (2.7) is ergodic over $E^{\mathcal{U}}$ [34] and $w_i^{\mathcal{U}}$ is equal to the proportion of time the system spends in state $P_i^{\mathcal{U}}$. The ensemble $E^{\mathcal{U}}$ represents ρ_{ss} in that

$$\sum_i w_i^{\mathcal{U}} P_i^{\mathcal{U}} = \rho_{ss}, \quad (2.12)$$

as guaranteed by Eq. (2.10).

3. Continuous Markovian Unravelings

The search for the most robust unraveling requires a search through the set, call it J , of all possible unravelings. This set is extremely large. Although the stochasticity in the superoperators \mathcal{U} can always be written in terms of quantum jumps, these jumps range in size from being infinitesimal, to being so large that the system state after the jump is always orthogonal to that before the

jump [35]. Also the unraveling need not be Markovian, even though the master equation is [36].

For this reason it is useful to consider a smaller (but still continuously infinite) set J' containing only continuous Markovian unravelings. A continuous (but not differentiable) time evolution arises from infinitely small (and infinitely frequent) jumps [26,36]. In this case the probability distribution for the pure states obeying the SME satisfies a Fokker-Planck equation [33]. On this basis it has been argued that these unravelings are the natural ones to consider for quantum systems expected to show quasi-classical behaviour [35].

For the general master equation (2.1) the elements \mathcal{U}' of J' can be written as

$$\mathcal{U}' dt = \sum_{k=1}^K \mathcal{H}[dW_k^*(t)c_k]. \quad (2.13)$$

Here $\mathcal{H}[A]$ is a nonlinear superoperator defined (for arbitrary operators A, B) by

$$\mathcal{H}[A]B \equiv AB + BA^\dagger - \text{Tr}[AB + BA^\dagger]B, \quad (2.14)$$

and the $dW_k(t)$ are the infinitesimal increments of a complex multi-dimensional Wiener process [33] satisfying

$$dW_j(t)dW_k^*(t) = dt \delta_{jk}, \quad (2.15)$$

$$dW_j(t)dW_k(t) = dt u_{jk}, \quad (2.16)$$

where the u_{jk} are arbitrary complex numbers obeying $|u_{jk}| \leq 1$ and $u_{jk} = u_{kj}$.

Some insight into the measurement parameters u_{jk} may be found by considering the simple case with one irreversible term; that is, $K = 1$ so that there is just one u . For specificity, say the system is an optical cavity with damping through one end mirror. Then the continuous Markovian unravelings correspond to two independent homodyne detection apparatuses [26], each of efficiency 1/2. If the local oscillator phases are θ_1 and θ_2 then $u = (e^{2i\theta_1} + e^{2i\theta_2})/2$. Thus if the two local oscillator phases are chosen to be identical then both apparatuses measure the same quadrature of the cavity mode and $|u|^2 = 1$, while in general $|u|^2 < 1$. For $u \neq 0$, different amounts of information are obtained about the cavity-field quadrature amplitudes and this tends to reduce the cavity field to a state with correspondingly different quadrature amplitude uncertainties.

For a master equation with K Lindblad terms the problem of finding the maximally robust unraveling in J' reduces to a search over the bounded region $\{u_{jk} : |u_{jk}|^2 \leq 1\}_{jk}$ in $K(K+1)$ -dimensional Euclidean space. Even for a moderately sized K (for example $K = 3$ is needed for the atom laser problem), this is a surprisingly large space which is difficult to search efficiently. For that reason we adopt in this paper a different search strategy which will be explained in Sec. IV A 2.

C. Quantifying the Robustness

1. Survival Probability

Imagine that the system has been evolving under a particular unraveling \mathcal{U} from an initial state at time $-\infty$ to the stationary ensemble at the present time 0. It will then be in the state $P_i^{\mathcal{U}}$ with probability $w_i^{\mathcal{U}}$. If we now cease to monitor the system then the state will no longer remain pure, but rather will relax toward ρ_{ss} under the evolution of Eq. (2.1).

This relaxation to equilibrium will occur at different rates for different states. For example, some unravelings will tend to collapse the system into a pure state that is very fragile, in that it quickly decoheres. In this case the ensemble would rapidly become a poor representation of the observer's expected knowledge about the system. Hence we can say that such an ensemble is a "bad" or "unnatural" representation of ρ . Conversely, an unravelling that produces robust states would remain an accurate description for a relatively long time. We expect such a "good" or "natural" ensemble to give more intuition about the dynamics of the system. The most robust ensemble we interpret as the "best" or "most natural" such ensemble.

We quantify the *robustness* of a particular state $P_i^{\mathcal{U}}$ by its survival probability $S_i^{\mathcal{U}}(t)$. This is the probability that the system would be found (by a hypothetical projective measurement) to still be in the state $P_i^{\mathcal{U}}$ at time t . It is given by [37]

$$S_i^{\mathcal{U}}(t) = \text{Tr}[P_i^{\mathcal{U}} e^{\mathcal{L}t} P_i^{\mathcal{U}}]. \quad (2.17)$$

Since we are considering an ensemble $E^{\mathcal{U}}$ we must define the average survival probability

$$S^{\mathcal{U}}(t) = \sum_i w_i^{\mathcal{U}} S_i^{\mathcal{U}}(t). \quad (2.18)$$

In the limit $t \rightarrow \infty$ the ensemble-averaged survival probability will tend towards the stationary value

$$S^{\mathcal{U}}(\infty) = \text{Tr}[\rho_{ss}^2]. \quad (2.19)$$

This is independent of the unravelling \mathcal{U} and is a measure of the mixedness of ρ_{ss} .

2. Comparison with Purity

As noted in Sec. II A 3 above, it is more common in discussions of robustness to use purity rather than survival probability. The purity of a state at time t can be quantified as

$$p_i^{\mathcal{U}}(t) = \text{Tr}[(e^{\mathcal{L}t} P_i^{\mathcal{U}})^2]. \quad (2.20)$$

The ensemble average of this quantity is also initially unity, and approaches $\text{Tr}[\rho_{ss}^2]$ as $t \rightarrow \infty$. Alternatively,

the purity could be quantified as the maximum overlap of any pure state $\tilde{P}_i(t)$ with the evolved mixed state:

$$\tilde{p}_i^{\mathcal{U}}(t) = \max_{\tilde{P}_i(t)} \text{Tr}[\tilde{P}_i(t) (e^{\mathcal{L}t} P_i^{\mathcal{U}})]. \quad (2.21)$$

For Gaussian states (see Sec. III) these quantities are simply related by $\tilde{p}_i^{\mathcal{U}}(t) = 2/[1 + 1/p_i^{\mathcal{U}}(t)]$.

We prefer to use the survival probability in this paper for the following reasons. First, we motivated our robustness criterion from the desire for $E^{\mathcal{U}}$ to *remain* a good description of the system once the unraveling ceases. That is, we wish to be able to usefully regard the members of the ensemble $E^{\mathcal{U}}$ as the states the system is “really” in at steady state. This is better quantified by the survival probability because the purity effectively takes into account only how close the state $e^{\mathcal{L}t} P_i$ remains to some pure state $\tilde{P}_i(t)$ [introduced in Eq. (2.21)], not how close it remains to the original state P_i . An ensemble constructed by considering the purity would thus in general only remain a good description of the system by including the deterministic (but not necessarily unitary) evolution of its members from P_i to $\tilde{P}_i(t)$ after the unraveling ceases. This time evolution would negate the idea that the ensemble of states P_i is the best representation of the system at steady state.

Another reason for preferring the survival probability comes from imagining that the unraveling \mathcal{U} continues after $t = 0$. In that case the survival probability $S_i^{\mathcal{U}}(t)$ could still be interpreted as the probability for the system to be found in its original state. By contrast the purity of the unraveled state would always be unity.

The final reason for preferring survival probability, already noted in Sec. II A 3, is that it yields results for the atom laser which have a clear and simple physical interpretation. We will show that this is so in the discussion section.

One limit in which quite different results are to be expected from using purity rather than survival probability is that in which the Hamiltonian part of the dynamics dominates. As will be shown, this limit is highly relevant for the atom laser.

Formally, we split the Liouvillian superoperator \mathcal{L} as

$$\mathcal{L} = \mathcal{L}_{\text{irr}} + \chi \mathcal{L}_{\text{rev}}, \quad (2.22)$$

where χ is a large parameter and

$$\mathcal{L}_{\text{irr}} \rho = \sum_{k=1}^K \mathcal{D}[c_k] \rho. \quad (2.23)$$

$$\mathcal{L}_{\text{rev}} \rho = -i[H, \rho]. \quad (2.24)$$

The reversibility of \mathcal{L}_{rev} implies that

$$\text{Tr}[A \mathcal{L}_{\text{rev}} B] = -\text{Tr}[B \mathcal{L}_{\text{rev}} A]. \quad (2.25)$$

To first order in time, both the survival probability and the purity depend only upon the irreversible term:

$$S(t) = 1 + t \text{Tr}[P \mathcal{L}_{\text{irr}} P], \quad (2.26)$$

$$p(t) = 1 + 2t \text{Tr}[P \mathcal{L}_{\text{irr}} P]. \quad (2.27)$$

For longer times both expressions will (in general) be dominated by the reversible term, but in different ways:

$$S(t) \simeq 1 + \chi^2 (t^2/2) \text{Tr}[P \mathcal{L}_{\text{rev}}^2 P], \quad (2.28)$$

$$p(t) \simeq 1 + \chi t^2 \text{Tr}[P(\mathcal{L}_{\text{irr}} \mathcal{L}_{\text{rev}} - \mathcal{L}_{\text{rev}} \mathcal{L}_{\text{irr}}) P]. \quad (2.29)$$

The Hamiltonian term directly affects the survival probability, but it affects the purity only in combination with the irreversible term.

3. Survival Time

The above analysis shows that the difference between purity and survival probability only shows up at finite times. Thus the best way to characterize robustness is to look not at the initial rate of decay of the survival probability, but at the time it takes to fall below some threshold value Λ satisfying

$$1 > \Lambda > \text{Tr}[\rho_{\text{ss}}^2]. \quad (2.30)$$

The ensemble-averaged survival time for a particular unraveling would then be defined as

$$\tau^{\mathcal{U}} = \min\{t : S^{\mathcal{U}}(t) = \Lambda\}. \quad (2.31)$$

Note that this time is the *first* time for which $S^{\mathcal{U}}(t) = \Lambda$. The survival probability is not necessarily monotonically decreasing and in some simple examples there will be many solutions to the equation $S^{\mathcal{U}}(t) = \Lambda$.

A natural choice of Λ , suggested in Ref. [21], is the maximum eigenvalue of ρ_{ss} :

$$\Lambda = \lim_{n \rightarrow \infty} (\text{Tr}[\rho_{\text{ss}}^n])^{1/n} \quad (2.32)$$

$$= \max\{\lambda \in \mathbb{R} : \rho_{\text{ss}} Q_{\lambda} = \lambda Q_{\lambda} = \lambda Q_{\lambda}^2\}. \quad (2.33)$$

This can be shown to satisfy $\Lambda > \text{Tr}[\rho_{\text{ss}}^2]$ as follows. Let the eigenvalues of ρ_{ss} be (in descending order), $\Lambda, \lambda_1, \lambda_2, \dots$. Then

$$\text{Tr}[\rho_{\text{ss}}^2] = \Lambda^2 + \sum_i \lambda_i^2 \quad (2.34)$$

$$< \Lambda^2 + \sum_i \Lambda \lambda_i \quad (2.35)$$

$$= \Lambda^2 + \Lambda(1 - \Lambda) = \Lambda. \quad (2.36)$$

Here the strict inequality holds unless all eigenvalues of ρ_{ss} are equal.

In the absence of any monitoring of the bath, the projector Q_{Λ} would be one’s best guess for what pure state the system is in at steady state. The chance of this guess being correct is simply Λ , which is obviously independent of time t . Using this Λ , the survival time $\tau^{\mathcal{U}}$ could thus be interpreted as the time at which the initial state $P_i^{\mathcal{U}}$

ceases (on average) to be any better than Q_Λ as an estimate of which pure state is occupied. In other words, the ensemble E^U is obsolete at time τ^U .

In this paper we do not use this choice for Λ , for reasons to be explained later. This brings a certain degree of arbitrariness into the analysis. However, as we show, the most important and interesting results we obtain are independent of the choice of Λ .

Having chosen a particular value for Λ , the survival time τ^U quantifies the robustness of an unraveling U . Let the set of all unravelings be denoted J as above. Then the subset of *maximally robust* unravelings J_M is

$$J_M = \{\mathcal{R} \in J : \tau^{\mathcal{R}} \geq \tau^U \forall U \in J\}. \quad (2.37)$$

As noted above, in practice it may be necessary to restrict the analysis to continuous Markovian unravelings J' , and the corresponding subset J'_M . Even if J_M has many elements $\mathcal{R}_1, \mathcal{R}_2, \dots$, these different unravelings may give the same ensemble $E^{\mathcal{R}} = E^{\mathcal{R}_1} = E^{\mathcal{R}_2} = \dots$. In this case $E^{\mathcal{R}}$ is the most natural ensemble representation of the stationary solution of a given master equation.

III. THE (ATOM) LASER

The system we wish to consider in this paper is the (atom) laser. As noted in the introduction, we take a laser to be a device which produces a coherent output, in the sense explained in Ref. [3]. An atom laser is thus a device which produces a coherent beam of bosonic atoms, analogous to the coherent beam of photons from an optical laser.

A. The Master Equation

A generic model for a laser was derived in Ref. [3]. It describes a single-mode field having annihilation operator a , evolving under linear damping and nonlinear amplification. The nonlinearity in the amplification is due to depletion of the source (the gain medium in optical lasers) and is essential for a coherent output to form. In the interaction picture, and measuring time in units of the decay rate, the master equation is

$$\dot{\rho} = \mu \mathcal{D}[a^\dagger] (\mathcal{A}[a^\dagger] + n_s)^{-1} \rho + \mathcal{D}[a]\rho. \quad (3.1)$$

The two terms on the right describe saturated gain and the decay due to the coupling of the laser mode to the output beam, respectively. Here n_s is the saturation boson number, μ is a (typically) large parameter, \mathcal{D} is as defined in Eq. (2.2) and for arbitrary operators A and B ,

$$\mathcal{A}[A]B = [A^\dagger AB + BA^\dagger A]/2. \quad (3.2)$$

For simplicity we take the limit where n_s can be ignored compared to aa^\dagger . Strictly this requires the limit

$n_s \ll 1$, because the smallest eigenvalue of aa^\dagger is 1. However, for a laser at steady state the mean boson number is typically much greater than 1, and only boson numbers close to the mean are occupied with any significant probability. In the above model the mean number is approximately $\mu - n_s$ in the limit of large μ . Hence in the limit $\mu \gg n_s, 1$ we can ignore n_s in the laser master equation.

Having made this simplification we now introduce more terms into Eq. (3.1) in order to create a more realistic model. First, we introduce a term describing phase diffusion. This will be present in optical lasers for all sorts of technical reasons such as thermal motion of the cavity mirrors. In an atom laser it may also be present for more fundamental reasons, such as collisions between uncondensed atoms (in the source modes) and atoms in the laser mode condensate. Treating this phase diffusion as a Markovian process, it is described by a Lindblad superoperator of the form $N\mathcal{D}[a^\dagger a]$, where N is the phase diffusion rate in units of the decay rate.

The second new term we introduce is peculiar to atom lasers: the self-energy of atoms in the condensate. This is described by a Hamiltonian equal to $\hbar C(a^\dagger a)^2$, with

$$C = \frac{2\pi\hbar a_s}{\kappa m} \int d^3\mathbf{r} |\psi(\mathbf{r})|^4, \quad (3.3)$$

where $\psi(\mathbf{r})$ is the wavefunction for the condensate mode, a_s is the s -wave scattering length, and κ is the unit-valued decay rate of the condensate. Like the extra phase diffusion term, this term has no effect on boson number; it only affects the phase of the field. However it is strictly not a phase diffusion term, but rather a dispersive term. It would arise in an optical laser containing a medium with a nonlinear refractive index.

Putting the four terms (gain, loss, phase diffusion and self-energy) together, the total master equation is

$$\dot{\rho} = (\mu \mathcal{D}[a^\dagger] \mathcal{A}[a^\dagger]^{-1} + \mathcal{D}[a] + N\mathcal{D}[a^\dagger a]) \rho - iC[(a^\dagger a)^2, \rho]. \quad (3.4)$$

That this is of the Lindblad form follows from the identity

$$\mathcal{D}[a^\dagger] \mathcal{A}[a^\dagger]^{-1} = \int_0^\infty dq \mathcal{D}[a^\dagger] e^{-qa^\dagger/2}. \quad (3.5)$$

The stationary solution is a Poissonian mixture of number states with mean μ , just as expressed in Eqs. (1.1) and (1.2):

$$\rho_{ss} = \int \frac{d\phi}{2\pi} \left| \sqrt{\mu} e^{i\phi} \right\rangle \left\langle \left| \sqrt{\mu} e^{i\phi} \right| \right| = \sum_{n=0}^{\infty} e^{-\mu} \frac{\mu^n}{n!} |n\rangle \langle n|. \quad (3.6)$$

1. The Linearized Master Equation

The master equation (3.4) is rather difficult to deal with because of the nonlinearities in both the gain term and the self-energy term. To make it more tractable we linearize this equation for a state localized about a mean field $\langle a \rangle = \sqrt{\mu}$. We make the replacement

$$a = \sqrt{\mu} + (x + iy)/2 \quad (3.7)$$

and get, to second order in x and y ,

$$\dot{\rho} = (1/4) \{ \mathcal{D}[x + iy] + (1 + \nu)\mathcal{D}[x] + \mathcal{D}[y] + \mathcal{H}[i(xy + yx)/2 - i\chi x^2] \} \rho, \quad (3.8)$$

where

$$\nu = 4N\mu \geq 0, \quad \chi = 4\mu C. \quad (3.9)$$

We have ignored a contribution to the linearized Hamiltonian which is proportional to $a^\dagger a$ as this simply indicates a frequency shift which can be removed in the interaction picture.

To solve this master equation, we use the Wigner representation $W(x, y)$ [27]. We make a Gaussian ansatz

$$W(x, y) = \exp \left[\frac{\mu_{20}\mu_{02}}{\mu_{20}\mu_{02} - \mu_{11}^2} \left(-\frac{(x - \mu_{10})^2}{2\mu_{20}} + \frac{\mu_{11}(x - \mu_{10})(y - \mu_{01})}{\mu_{20}\mu_{02}} - \frac{(y - \mu_{01})^2}{2\mu_{02}} \right) \right] \div \left(2\pi\sqrt{\mu_{20}\mu_{02} - \mu_{11}^2} \right). \quad (3.10)$$

Substituting this into Eq. (3.8) yields the following ODEs for the moments

$$\dot{\mu}_{10} = -\mu_{10}, \quad (3.11)$$

$$\dot{\mu}_{01} = -\chi\mu_{10}, \quad (3.12)$$

$$\dot{\mu}_{20} = -2\mu_{20} + 2, \quad (3.13)$$

$$\dot{\mu}_{11} = -\mu_{11} - \chi\mu_{20}, \quad (3.14)$$

$$\dot{\mu}_{02} = -2\chi\mu_{11} + 2 + \nu. \quad (3.15)$$

The solution is easy to find

$$\mu_{10}(t) = \mu_{10}(0)w, \quad (3.16)$$

$$\mu_{01}(t) = \mu_{01}(0) - \chi\mu_{10}(0)(1 - w), \quad (3.17)$$

$$\mu_{20}(t) = \mu_{20}(0)w^2 + 1 - w^2, \quad (3.18)$$

$$\mu_{11}(t) = \mu_{11}(0)w - \chi \{ 1 + w[\mu_{20}(0) - 2] + w^2[1 - \mu_{20}(0)] \}, \quad (3.19)$$

$$\begin{aligned} \mu_{02}(t) = & \mu_{02}(0) + (2 + \nu)t - 2\chi\mu_{11}(0)(1 - w) \\ & + 2\chi^2 \{ t + [\mu_{20}(0) - 2](1 - w) \\ & + [1 - \mu_{20}(0)](1 - w^2)/2 \}. \end{aligned} \quad (3.20)$$

Here we are using the abbreviation $w \equiv e^{-t}$.

2. Coherence

Having solved for the dynamics of our (atom) laser model, we can now answer the question, is it a true laser. That is, does it satisfy the criteria for a coherent output as detailed in Ref. [3]. The first two criteria will be satisfied provided the output coupling is realized in a suitable way. The next two relate to the quantum noise of the state, and depend upon the dynamics.

First, the laser intensity should be well-defined. Although this criterion is strictly defined in terms of the output of the laser, it will be satisfied if the boson number of the laser mode itself is well-defined. In the present case this is clearly so provided the mean number satisfies

$$\mu \gg 1, \quad (3.21)$$

as the standard deviation in the boson number is equal to $\sqrt{\mu}$.

Second, the laser phase should be well-defined in the sense that the phase should stay approximately constant over the time between the emission of one boson and the next. With a unit damping rate, this time is equal to μ^{-1} . Rigorously, we require that the magnitude of the first order coherence function

$$g^{(1)}(t) = \frac{\langle a^\dagger(t)a(0) \rangle}{\langle a^\dagger a \rangle} \quad (3.22)$$

remain close to unity for $t = \mu^{-1}$. For a laser which has a Poissonian number distribution, this is exactly equivalent to requiring that the system, initially in a coherent state of mean number μ , still have a phase variance much less than unity after a time $t = \mu^{-1}$.

Without loss of generality we can take the initial coherent state to be $|\sqrt{\mu}\rangle$. Then $\mu_{10}(0) = \mu_{01}(0) = \mu_{11}(0) = 0$, $\mu_{20} = \mu_{02} = 1$, and y is the phase quadrature. Assuming that the phase uncertainty remains relatively small, we can make the approximation

$$\phi = \frac{y}{2\sqrt{\mu}}. \quad (3.23)$$

From Eq. (3.17), the mean phase remains zero

$$\langle \phi(t) \rangle = \frac{\mu_{01}(t)}{2\sqrt{\mu}} = 0 \quad (3.24)$$

while the phase variance increases as

$$\langle \phi^2(t) \rangle = \frac{\mu_{02}(t)}{4\mu}. \quad (3.25)$$

Substituting $t = \mu^{-1} \ll 1$ into Eq. (3.20) yields

$$\langle \phi^2(t) \rangle = \frac{1 + (2 + \nu)\mu^{-1} + \chi^2\mu^{-2}}{4\mu}. \quad (3.26)$$

For the phase to remain well-defined we require this to be much less than unity. Since we already require $\mu \gg 1$, this gives the extra conditions

$$\chi \ll \mu^{3/2}, \quad (3.27)$$

$$\nu \ll \mu^2. \quad (3.28)$$

In a typical optical laser (and certainly in some models of atom lasers [10]), $\nu \gg 1$. This means that excess phase diffusion dominates the intrinsic phase diffusion (which gives the 2 in the $2 + \nu$ term). In a typical atom laser, it is also likely that excess phase diffusion will dominate. However, as long as $\nu \ll \mu^2$ the laser will remain coherent. Since $\nu = 4N\mu$, this is equivalent to the condition

$$N \ll \mu. \quad (3.29)$$

This expression places an upper bound on the phase diffusion rate N for the device to be considered a laser.

For an optical laser any nonlinear refractive index is usually small and $\chi \ll 1$. For an atom laser χ is likely to be much greater than one. To be a true atom laser it is necessary for it to remain much less than $\mu^{3/2}$. Since $\chi = 4\mu C$ the phase coherence condition places an upper bound on the condensate self-energy in Eq. (3.3) of

$$C \ll \mu^{1/2}. \quad (3.30)$$

IV. MRU OF THE (ATOM) LASER

A. Physically Realizable Ensembles

We now wish to consider monitoring the environment of the laser in order to realize physically an ensemble of pure states. This would be very difficult to do experimentally, as it would require monitoring all reservoirs for the device, including the source of bosons (the gain

medium) and the sources of phase diffusion as well as the laser output. However in principal these things can be done providing the laser evolution is well-approximated by a Markovian master equation.

1. The Stochastic Master Equation

As mentioned in Sec. II B 3, we will restrict ourselves to continuous Markovian unravelings. From the master equation (3.4) in the Lindblad form (3.5), the stochastic master equation (SME) for the projector P representing the system state is

$$\begin{aligned} dP = & dt \left\{ \mu \int_0^\infty dq \mathcal{D}[a^\dagger e^{-qaa^\dagger/2}] + \mathcal{D}[a] + N \mathcal{D}[a^\dagger a] \right\} P \\ & + \sqrt{\mu} \int_0^\infty dq \mathcal{H}[dW_q^*(t) a^\dagger e^{-qaa^\dagger/2}] P \\ & + \mathcal{H}[dW_0^*(t) a] P + \sqrt{N} \mathcal{H}[dW_N^*(t) a^\dagger] P \\ & - idt [C(a^\dagger a)^2, P]. \end{aligned} \quad (4.1)$$

Here dW_0 is a zero-mean white noise term. If we define $\zeta_0(t) = dW_0(t)/dt$ we have

$$E[\zeta_0^*(t) \zeta_0(t')] = \delta(t - t'). \quad (4.2)$$

and likewise for ζ_N and ζ_q for each q . We say that these white noise terms are *distinct* because the cross terms are zero, for example

$$E[\zeta_0^*(t) \zeta_N(t')] = 0. \quad (4.3)$$

Now we wish to linearize. First note that

$$\sqrt{\mu} \int_0^\infty dq \zeta_q^*(t) a^\dagger \exp(-qaa^\dagger/2) \simeq \sqrt{\mu} \int_0^\infty dq \zeta_q^*(t) e^{-\mu q/2} \sqrt{\mu} [1 + (x + iy - \mu xq)/2\sqrt{\mu}] \quad (4.4)$$

$$= c\text{-number} + \frac{y}{2} \int_0^\infty dq i \zeta_q^*(t) e^{-\mu q/2} + \frac{x}{2} \int_0^\infty dq \zeta_q^*(t) e^{-\mu q/2} (1 - q) \quad (4.5)$$

$$= c\text{-number} + [y \zeta_2^*(t) + x \zeta_3^*(t)]/2, \quad (4.6)$$

where $\zeta_2(t)$ and $\zeta_3(t)$ are distinct complex normalized white noise terms as usual.

Using this, we can linearize Eq. (4.1) as

$$\begin{aligned} dP = & (1/4) dt \left\{ \mathcal{D}[x + iy]\rho + (1 + \nu)\mathcal{D}[x]\rho + \mathcal{D}[y]\rho + \mathcal{H}[i(xy + yx)/2] + \mathcal{H}[-i\chi x^2] \right\} P \\ & + (1/2) \left\{ \mathcal{H}[dW_0^*(t)(x + iy)] + \sqrt{1 + \nu} \mathcal{H}[dW_1^*(t)x] + \mathcal{H}[dW_2^*(t)y] \right\} P. \end{aligned} \quad (4.7)$$

where we have defined a new white noise source $\sqrt{1 + \nu} dW_1(t) = dW_3(t) + \sqrt{\nu} dW_N(t)$. We could have obtained this result directly from the linearized form of the master equation (3.8), but this derivation makes the physical origin of the noise terms apparent.

The three complex white noise sources $dW_j = \zeta_j dt$ are distinct in the above sense that

$$E[\zeta_i^*(t) \zeta_j(t')] = \delta_{ij} \delta(t - t'). \quad (4.8)$$

However they can still be correlated in the sense that

$$E[\zeta_i(t) \zeta_j(t')] = u_{ij} \delta(t - t'), \quad (4.9)$$

where the $u_{ij} = u_{ji}$ are arbitrary complex numbers with norm less than or equal to unity. The δ -function in time

in Eq. (4.9) is not required to reproduce the master equation. It is a consequence of our restriction to Markovian unravelings.

Now it is a remarkable fact about the stochastic master equation (4.7) that it takes Gaussian states to Gaussian states. This will be true for any stochastic master equa-

tion which is at most second-order in x or y and which describes continuous measurements. The significance in this case is that we can again use the ansatz (3.10), and we need only the equations of motion for the five moments. We find the following equations (to be interpreted in the Itô sense [33])

$$\dot{\mu}_{10} = -\mu_{10} + \text{Re} \{ \zeta_0^*(t) [\mu_{20} - 1 + i\mu_{11}] + \zeta_1^*(t) \sqrt{1+\nu} [\mu_{20}] + \zeta_2^*(t) [\mu_{11} + i] \} \quad (4.10)$$

$$\dot{\mu}_{01} = -\chi\mu_{10} + \text{Re} \{ \zeta_0^*(t) [i\mu_{02} - i + \mu_{11}] + \zeta_1^*(t) \sqrt{1+\nu} [\mu_{11} - i] + \zeta_2^*(t) [\mu_{02}] \} \quad (4.11)$$

$$\begin{aligned} \dot{\mu}_{20} = & 2 - 2\mu_{20} - \text{Re} [(\mu_{20} - 1)^2 + \mu_{11}^2 + (1 + \nu)\mu_{20}^2 + \mu_{11}^2 + 1 \\ & + u_{00}^*(\mu_{20} - 1 + i\mu_{11})^2 + u_{11}^*(1 + \nu)\mu_{20}^2 + u_{22}^*(\mu_{11} + i)^2 \\ & + 2u_{01}^*\sqrt{1+\nu}(\mu_{20} - 1 + i\mu_{11})\mu_{20} + 2u_{02}^*(\mu_{20} - 1 + i\mu_{11})(\mu_{11} + i) + 2u_{12}^*\sqrt{1+\nu}(\mu_{11} + i)\mu_{20}] / 2 \end{aligned} \quad (4.12)$$

$$\begin{aligned} \dot{\mu}_{02} = & -2\chi\mu_{11} + 2 + \nu - \text{Re} [(\mu_{02} - 1)^2 + \mu_{11}^2 + (1 + \nu)(\mu_{11}^2 + 1) + \mu_{02}^2 \\ & + u_{00}^*(i\mu_{02} - i + \mu_{11})^2 + u_{11}^*(1 + \nu)(\mu_{11} - i)^2 + u_{22}^*\mu_{02}^2 \\ & + 2u_{01}^*\sqrt{1+\nu}(i\mu_{02} - i + \mu_{11})(\mu_{11} - i) + 2u_{02}^*(i\mu_{02} - i + \mu_{11})\mu_{02} + 2u_{12}^*\sqrt{1+\nu}(\mu_{11} - i)\mu_{02}] / 2 \end{aligned} \quad (4.13)$$

$$\begin{aligned} \dot{\mu}_{11} = & -\mu_{11} - \chi\mu_{20} - \text{Re} \{ (\mu_{20} - 1 + i\mu_{11})(-i\mu_{02} + i + \mu_{11}) + (1 + \nu)(\mu_{11} - i)\mu_{20} + \mu_{02}(\mu_{11} - i) \\ & + u_{00}^*(\mu_{20} - 1 + i\mu_{11})(i\mu_{02} - i + \mu_{11}) + u_{11}^*(1 + \nu)\mu_{20}(\mu_{11} - i) + u_{22}^*\mu_{02}(\mu_{11} + i) \\ & + u_{01}^*\sqrt{1+\nu}[(\mu_{20} - 1 + i\mu_{11})(\mu_{11} - i) + \mu_{20}(i\mu_{02} - i + \mu_{11})] + u_{12}^*\sqrt{1+\nu}[\mu_{20}\mu_{02} + (\mu_{11} + i)(\mu_{11} - i)] \\ & + u_{02}^*[(i\mu_{02} - i + \mu_{11})(\mu_{11} + i) + (\mu_{20} - 1 + i\mu_{11})\mu_{02}] \} / 2 \end{aligned} \quad (4.14)$$

2. The Stationary Solutions

From these equations we see that the evolution of the second order moments $\mu_{20}, \mu_{02}, \mu_{11}$ is deterministic. This means that for a given unraveling \mathcal{U} the stationary ensemble will consist of Gaussian pure states all having the same second order moments. They are distinguished only by their first order moments $\bar{x} = \mu_{10}, \bar{y} = \mu_{01}$, which therefore take the role of the index i in Eq. (2.11). The different ensembles themselves are indexed by another pair of numbers, μ_{11}, μ_{20} which play the role of \mathcal{U} in Eq. (2.11). We do not need μ_{02} because the purity of the unraveled states implies that

$$\mu_{20}\mu_{02} - \mu_{11}^2 = 1. \quad (4.15)$$

However, it should be noted that the mapping from \mathcal{U} to μ_{11}, μ_{20} is in general many-to-one as discussed below.

We now introduce a new notation for the second order moments,

$$\alpha = \frac{\mu_{02}}{\mu_{20}\mu_{02} - \mu_{11}^2}, \quad (4.16)$$

$$\beta = \frac{\mu_{11}}{\mu_{20}\mu_{02} - \mu_{11}^2}, \quad (4.17)$$

$$\gamma = \frac{\mu_{20}}{\mu_{20}\mu_{02} - \mu_{11}^2}. \quad (4.18)$$

For pure states satisfying Eq. (4.15), we have simply

$$\alpha = \mu_{02}; \beta = \mu_{11}; \gamma = \mu_{20}, \quad (4.19)$$

The different ensembles are now indexed by the pair β, γ .

Of course not all pairs β, γ correspond to physically realizable ensembles. Since the ensemble we are considering has evolved to a steady state at $t = 0$, the only valid pairs must satisfy Eqs. (4.12)–(4.14) with the left-hand sides set to zero. This gives three simultaneous equations which, on splitting u_{ij} into real r_{ij} and imaginary h_{ij} components, can be written as

$$\begin{aligned} 1 - \gamma - (1 + \nu/2)\gamma^2 - \beta^2 = & r_{00}[(\gamma - 1)^2 - \beta^2]/2 + r_{11}(1 + \nu)\gamma^2/2 + r_{22}(\beta^2 - 1)/2 \\ & + h_{00}\beta(\gamma - 1) + h_{22}\beta \\ & + r_{01}\sqrt{1+\nu}\gamma(\gamma - 1) + r_{02}(\gamma - 2)\beta + r_{12}\sqrt{1+\nu}\gamma\beta \\ & + h_{01}\sqrt{1+\nu}\gamma\beta + h_{02}(\beta^2 + \gamma - 1) + h_{12}\sqrt{1+\nu}\gamma\beta \end{aligned} \quad (4.20)$$

$$\begin{aligned} -2\chi\beta + (1 + \nu/2)(1 - \beta^2) - \alpha^2 + \alpha = & r_{00}[\beta^2 - (\alpha - 1)^2]/2 + r_{11}(1 + \nu)(\beta^2 - 1)/2 + r_{22}\alpha^2/2 \\ & + h_{00}\beta(\alpha - 1) + h_{11}(1 + \nu)(-\beta) \\ & + r_{01}\sqrt{1+\nu}(\beta^2 + \alpha - 1) + r_{02}\beta\alpha + r_{12}\sqrt{1+\nu}\beta\alpha \\ & + h_{01}\sqrt{1+\nu}(\alpha - 2)\beta + h_{02}(\alpha - 1)\alpha + h_{12}\sqrt{1+\nu}(-\alpha) \end{aligned} \quad (4.21)$$

$$-\chi\gamma - \alpha\beta - (1 + \nu/2)\gamma\beta = r_{00}\beta(\gamma - \alpha)/2 + r_{11}(1 + \nu)\gamma\beta/2 + r_{22}\beta\alpha/2$$

$$\begin{aligned}
& + h_{00}[\beta^2 + (\alpha - 1)(\gamma - 1)]/2 + h_{11}(1 + \nu)(-\gamma)/2 + h_{22}\alpha/2 \\
& + r_{01}\sqrt{1 + \nu}\gamma\beta + r_{02}[\beta^2 + 1 + (\gamma - 2)\alpha]/2 + r_{12}\sqrt{1 + \nu}(\alpha\gamma + \beta^2 + 1)/2 \\
& + h_{01}\sqrt{1 + \nu}[\beta^2 + 1 + (\alpha - 2)\gamma]/2 + h_{02}\beta\alpha,
\end{aligned} \tag{4.22}$$

where α is to be read as $(1 + \beta^2)/\gamma$.

These three equations are nonlinear in β, γ but linear in the 12 real variables r_{ij}, h_{ij} . This means that if the values of γ and β are known then the three equations can be solved for r_{ij}, h_{ij} . Since there are only three equations for the 12 unknown variables, the resulting linear system is non-singular and an (uncountably) infinite number of solutions are possible. We denote the family of such solutions $F_\xi = \{r_{ij}^{(\xi)}, h_{ij}^{(\xi)}\}_{ij}$, indexed by ξ . Physically this arises because many different unravelings \mathcal{U} may lead to the same steady state ensemble β, γ . The question of whether a given pair of values of γ and β represents a physically realizable state then becomes the problem of determining whether any of the solutions F_ξ satisfy the unit norm condition of the correlation coefficients $u_{ij}^{(\xi)} = r_{ij}^{(\xi)} + i h_{ij}^{(\xi)}$ in Eq. (4.9), that is, determining whether $|u_{ij}^{(\xi)}| \leq 1$ for all i, j for any value of ξ . This problem can be solved by finding the solution F_Ξ that gives the smallest value of the expression

$$\max_{ij} |u_{ij}^{(\xi)}| = \lim_{n \rightarrow \infty} \left[\sum_{ij} |u_{ij}^{(\xi)}|^n \right]^{1/n} \tag{4.23}$$

and then checking if $|u_{ij}^{(\Xi)}| \leq 1$ for all i, j . In practice we use a singular value decomposition routine to find the solution space $\{F_\xi\}_\xi$ and a value of $n = 50$ in Eq. (4.23) instead of the infinite limit; we estimate that this allows us to delineate the regions in the γ, β plane representing physically realizable states to within 0.3% of the value of γ and β .

3. The Stationary Ensemble

The stationary solution of the linearized master equation (3.8) has a Wigner function which is independent of phase (y) and has the following amplitude (x) dependence:

$$W_{ss}(x) \propto (2\pi)^{-1/2} \exp(-x^2/2). \tag{4.24}$$

This is as expected from the stationary solution of the full master equation, Eq. (3.6). A flat phase distribution linearizes into a flat y -distribution.

As shown above, the long-time solution of the SME (4.6) is an ensemble of Gaussian pure states in which the

second order moments $\mu_{20}, \mu_{11}, \mu_{02}$ are identical in all members of the ensemble, but $\bar{x} = \mu_{10}$ and $\bar{y} = \mu_{01}$ are allowed to vary. The ensemble is thus represented as

$$E^{\mathcal{U}} = \{w_{\bar{x}, \bar{y}}^{\mathcal{U}}, P_{\bar{x}, \bar{y}}^{\mathcal{U}}\}_{\bar{x}, \bar{y}}, \tag{4.25}$$

where the second order moments of the pure state $P_{\bar{x}, \bar{y}}^{\mathcal{U}}$ are determined by the unraveling \mathcal{U} .

The weighting function $w_{\bar{x}, \bar{y}}^{\mathcal{U}}$ for the members of the ensemble is Gaussian. This follows from the fact that Eqs. (4.10), (4.11) for \bar{x} and \bar{y} describe in steady state (where the second-order moments are constant) a two-dimensional Ornstein-Uhlenbeck process [33]. Such a process has a stationary probability distribution which is Gaussian.

Rather than deriving this stationary Gaussian distribution $w_{\bar{x}, \bar{y}}^{\mathcal{U}}$ from the Ornstein-Uhlenbeck process we can derive it more simply by noting that it must satisfy

$$\rho_{ss} = \int d\bar{x} d\bar{y} w_{\bar{x}, \bar{y}}^{\mathcal{U}} P_{\bar{x}, \bar{y}}^{\mathcal{U}}. \tag{4.26}$$

This is guaranteed by the fact that the SME is equivalent to the master equation on average. Evidently \bar{y} should always have a flat weighting distribution, and \bar{x} should have the weighting distribution

$$w^{\mathcal{U}}(\bar{x}) = [2\pi(1 - \mu_{20})]^{-1/2} \exp\left\{-\bar{x}^2/[2(1 - \mu_{20})]\right\}. \tag{4.27}$$

This ensures that

$$W_{ss}(x) \propto \int d\bar{y} \int d\bar{x} w^{\mathcal{U}}(\bar{x}) W_{\bar{x}, \bar{y}}^{\mathcal{U}}(x, y), \tag{4.28}$$

where $W_{\bar{x}, \bar{y}}^{\mathcal{U}}(x, y)$ is the Wigner function of $P_{\bar{x}, \bar{y}}^{\mathcal{U}}$.

B. Survival Probability

We are interested in the survival probability of the states with Wigner function $W_{\bar{x}, \bar{y}}^{\mathcal{U}}(x, y)$. Obviously this is independent of \bar{y} so we will drop this subscript, and set $\bar{y} = 0$ for ease of calculation. The state with initial moments $\mu_{ij}(0)$ will evolve to a state with moments $\mu_{ij}(t)$ given by (3.16–3.20). We will denote the former state $W_{\bar{x}}(x, y, 0)$ and the latter $W_{\bar{x}}(x, y, t)$. The survival probability of this state is given by

$$S_{\bar{x}}(t) \equiv \text{Tr}[P_{\bar{x}} e^{\mathcal{L}t} P_{\bar{x}}] = 4\pi \int dx dy W_{\bar{x}}(x, y, 0) W_{\bar{x}}(x, y, t) \tag{4.29}$$

$$= 4\pi \int dx dy \mathcal{N}(0) \exp\left[\frac{\mu_{20}(0)\mu_{02}(0)}{\mu_{20}(0)\mu_{02}(0) - \mu_{11}(0)^2} \left(-\frac{(x - \bar{x})^2}{2\mu_{20}(0)} + \frac{\mu_{11}(0)(x - \bar{x})y}{\mu_{20}(0)\mu_{02}(0)} - \frac{y^2}{2\mu_{02}(0)}\right)\right] \tag{4.30}$$

$$\times \mathcal{N}(t) \exp \left[\frac{\mu_{20}(t)\mu_{02}(t)}{\mu_{20}(t)\mu_{02}(t) - \mu_{11}(t)^2} \left(-\frac{(x - \bar{x}w)^2}{2\mu_{20}(t)} + \frac{\mu_{11}(t)(x - \bar{x}w)(y + \chi\bar{x}(1-w))}{\mu_{20}(t)\mu_{02}(t)} - \frac{(y + \chi\bar{x}(1-w))^2}{2\mu_{02}(t)} \right) \right],$$

where

$$\mathcal{N} = \left(2\pi \sqrt{\mu_{20}\mu_{02} - \mu_{11}^2} \right)^{-1}. \quad (4.31)$$

This survival probability should be averaged over all \bar{x} , weighted by the distribution (4.27) to get

$$S^U(t) = \int d\bar{x} S_{\bar{x}}(t) w^U(\bar{x}). \quad (4.32)$$

Thus $S(t)$ is given by a triple Gaussian integral which evaluates to the following:

$$S^U(t) = 2 \sqrt{\frac{(\alpha_t \gamma_t - \beta_t^2)/[1 + (1 - \gamma_0)R_t]}{(\alpha_0 + \alpha_t)(\gamma_0 + \gamma_t) - (\beta_0 + \beta_t)^2}} \quad (4.33)$$

where

$$\begin{aligned} R_t = \alpha_0 + \alpha_t w^2 + 2\beta_t \chi w z + \gamma_t \chi^2 z^2 - \frac{(\alpha_0 + \alpha_t w + \beta_t \chi z)^2}{\alpha_0 + \alpha_t} \\ - \frac{[(\beta_0 + \beta_t)(\alpha_0 + \alpha_t w + \beta_t \chi z) - (\alpha_0 + \alpha_t)(\beta_0 + \beta_t w + \gamma_t \chi z)]^2}{(\alpha_0 + \alpha_t)[(\alpha_0 + \alpha_t)(\gamma_0 + \gamma_t) - (\beta_0 + \beta_t)^2]}, \end{aligned} \quad (4.34)$$

where $z \equiv 1 - w$ and α, β, γ are as in Eqs. (4.16)–(4.18), and μ_{ij} are as in Eqs. (3.16)–(3.20). Note that at $t = 0$ the state is pure, so that $\alpha_0 = \mu_{02}, \beta_0 = \mu_{11}, \gamma_0 = \mu_{20}$ as previously.

The survival probability $S^U(t)$ is thus a function of the initial state parameters γ_0 and β_0 , and the dynamical parameters ν and χ . Because μ_{20} cannot be greater than one (the stationary variance in x), we also have the restriction $\gamma_0 \leq 1$. Other restrictions on γ_0 and β_0 come from the solution of the equations in Sec. IV A 2.

From these expressions it is evident that there would be a problem in choosing Eq. (4.38) for Λ (as suggested in Ref. [21]): it is very close to the value for $\text{Tr}[\rho_{ss}^2] = (4\pi\mu)^{-1/2}$. This means that the survival time would be equal to the time by which the system has relaxed almost to the equilibrium mixed state. In particular, its phase would necessarily be poorly defined by this time, which means that the linearization of the dynamics which we have been using would not be valid.

If instead we start with the solution (4.24) of the linearized dynamics, we have an even worse situation:

$$\text{Tr}[\rho_{ss}^2] = \lim_{n \rightarrow \infty} \sqrt[n]{\text{Tr}[\rho_{ss}^n]} = 0. \quad (4.39)$$

In this case the survival time would always be infinite, which is not helpful.

Because of these problems, we have not chosen the largest eigenvalue of ρ_{ss} for Λ . Instead we have investigated the dependence of τ^R on Λ for various values, namely $\Lambda = 0.5, 0.2, 0.1, 0.05$. As will be shown, the most robust ensemble, (that with the largest survival time) is substantially independent of Λ . Unless otherwise stated we choose Λ to be the midpoint of the two bounds in Eq. (4.36), namely

$$\Lambda = 1/2. \quad (4.40)$$

where Λ is a constant satisfying

$$1 > \Lambda > \text{Tr}[\rho_{ss}^2]. \quad (4.36)$$

From the solution (3.6) of the nonlinear dynamics, the lower bound on Λ is, for $\mu \gg 1$,

$$\text{Tr}[\rho_{ss}^2] = (4\pi\mu)^{-1/2}. \quad (4.37)$$

In the same limit, the largest eigenvalue for ρ_{ss} is

$$\lim_{n \rightarrow \infty} \sqrt[n]{\text{Tr}[\rho_{ss}^n]} = (2\pi\mu)^{-1/2}. \quad (4.38)$$

V. RESULTS

A. Varying χ

First we present the results for fixed ν to see the effect of varying χ . Because our results are numerical, we present them mostly in a graphical form.

1. Evolution at $\chi = 0$ and $\chi = 100$

Fig. 1 shows the evolution of various initially pure Gaussian quantum states under the master equation (3.8). We represent these states by the one standard-deviation ellipses of the Wigner function, the evolution of which is given by Eqs. (3.16)–(3.20). In each case we choose the initial mean location of the state in phase space to be $\bar{x} = \bar{y} = 0$ (except for the last in which additionally $\bar{x} = \pm 1$).

The first case in Fig. 1(a) is for $\nu = 0, \chi = 0$, and an initial coherent state. The ellipses are plotted for $t = 0, 3, 10$. The middle time is the ensemble-averaged survival time for an ensemble of coherent states; that is, the time at which the ensemble-averaged survival probability $S(t)$ drops to 1/2. For the particular case of the coherent state there is no distinction between the ensemble-averaged survival probability and the survival probability of a single coherent state $S_{\bar{x}}(t)$. That is because the x -variance γ of a coherent state is equal to the ensemble-averaged x -variance, namely unity. Note that the only dynamics in evidence here is phase diffusion, causing the y variance of the state to increase. For $\chi = \nu = 0$, the coherent state ensemble is in fact the maximally robust ensemble. This can be verified analytically.

The second case in Fig. 1(b) is again for an initial coherent state but with $\nu = 0, \chi = 100$, plotted for $t = 0, 0.0343, 0.1$. Again the middle time is the survival time for the coherent state. Note that it is two orders of magnitude smaller than the coherent state survival time for $\chi = 0$. The effect of the large χ is to rapidly shear the state. This is because the $a^{\dagger 2}a^2$ nonlinearity amounts to an intensity-dependent frequency shift. The coherent state ensemble, however, is not the most robust ensemble for $\chi = 100$.

The most robust ensemble for $\nu = 0, \chi = 100$, as determined by the numerical method discussed above, is the final case shown. Figure 1(c) displays three members, $\bar{x} = 0, \pm 1$, of this ensemble. Note that the $t = 0$ state is a highly amplitude-squeezed state. In fact it is not *exactly* amplitude-squeezed; the x - y covariance $\beta = \mu_{11}$ is equal to 0.177. In general, the angle θ between the major-axis of the ellipse and the y -axis is

$$\theta = \frac{1}{2} \arctan \frac{2\beta}{\alpha - \gamma} = \frac{1}{2} \arctan \frac{2\beta\gamma}{1 + \beta^2 - \gamma^2}. \quad (5.1)$$

In the limit of small γ and β this becomes $\theta \simeq \beta\gamma$. In this case, with $\gamma = 0.0613$, we have $\theta = 0.0105$ radians. This angle of rotation is almost too small to make out in the figure. It is nevertheless interesting that this slight

rotation is a persistent feature, and that it is actually in the opposite direction to the rotation caused by the shearing. That is, as the most robust state evolves it passes through a point where the squeezing is purely in the amplitude.

Because the x -variance γ of the states in this ensemble E^R is less than unity, the different members of E^R have different values of \bar{x} . The three initial states we show, with $\bar{x} = 0$ and $\bar{x} = \pm 1$, are typical members of the ensemble. The states into which these member of the maximally robust ensemble evolve are plotted for $t = 0.0612$ (the survival time) and $t = 0.1$ [as in Fig. 1(b)]. Note that the survival time is almost twice as large as for the coherent state ensemble in Fig. 1(b).

From Fig. 1 it is evident that the evolved state from the initial state with $\bar{x} = 0$ in the third case (c) at $t = 0.0612$ is much closer to its initial state than the evolved state in the second case (b) is at time $t = 0.0343$, even though both of these times are the survival time at which the survival probability drops to 1/2. However, the evolved states from the initial states with $\bar{x} = \pm 1$ in case (c) have a lower overlap with their initial states than does the evolved coherent state of case (b). This clearly illustrates that the survival probability is necessarily a property of the whole ensemble of states, not of a single member.

Figure 1 also shows that the survival probability decays for different reasons in different cases. In case (a) it decays because the evolved state becomes more mixed, due to phase diffusion. In case (b) it decays primarily because the evolved state changes shape (shearing) while remaining relatively pure. In case (c) it decays largely because the mean position of the evolved state moves away from that of the initial states in phase space.

In Fig. 2 we compare the ensemble-averaged survival probability $S(t)$ for the three cases in Fig. 1. Note that the time scale for case (a) differs from that used for cases (b) and (c). Curves (b) and (c) give $S(t)$ for the coherent state and maximally robust state ensembles, respectively, for $\nu = 0$ and $\chi = 100$. For short times the survival probability for the coherent state ensemble (b) is greater than the survival probability for the most robust ensemble (c). Indeed, the gradient of the survival probability for the coherent state ensemble at $t = 0$ is much less than that of the most robust ensemble. This underlines the importance of the survival time, rather than the initial rate of decay of survival probability, to quantify robustness.

At short times the survival probability generally decays linearly, due to irreversible processes, as discussed in Sec. II C 2. A coherent state minimizes this form of decoherence, resulting in an almost quadratic behaviour of $S^{|\alpha\rangle}(t)$ for $t \lesssim \chi^{-1} = 0.01$. This can be understood from the asymptotic analytical expression in Eq. (2.28) for the survival probability for a master equation with a large reversible term. This expression only applies for the survival probability of a single state, but is applicable to a coherent state ensemble because all members are effectively identical. It need not, and indeed does not, apply to the most robust ensemble. In comparison with

the coherent state ensemble, the most robust ensemble is affected more by irreversible evolution at short times but less by the interplay of reversible and irreversible terms at longer times.

2. MRU as a function of χ .

Having looked in detail at the most robust states for χ vanishing and χ large, we now present an overview for χ ranging from 1 to 1000. In Fig. 3 we plot the second-order moments $\alpha^R, \beta^R, \gamma^R$ defining the most robust ensemble E^R , as a function of χ . We also plot the survival time τ^R for this ensemble, and, for comparison, the survival time $\tau^{|\alpha\rangle}$ for an ensemble consisting of coherent states.

For values of χ less than about 2.7 the members of the most robust ensemble are close to coherent states, with $\alpha^R \approx \gamma^R = 1$ and $\beta^R \ll 1$. At $\chi \approx 2.7$ the curves change direction. The amplitude-quadrature variance γ remains equal to unity up to $\chi \approx 5.3$, while the phase-quadrature variance increases due to shearing of the ellipse. The greatest value of θ^R (as defined above) is about 30 degrees at $\chi \approx 5.3$. At this point, the curves change discontinuously, and as χ increases the squeezing of the most robust states becomes ever closer to pure amplitude-squeezing.

As χ becomes large, all of the curves plotted tend to straight lines on the log-log plot. It is thus an easy matter to read off the following power laws from the gradients of these lines:

$$\alpha^R \sim \chi^{2/3}, \quad (5.2)$$

$$\gamma^R \sim \chi^{-2/3}, \quad (5.3)$$

$$\beta^R \sim \chi^{-1/3}, \quad (5.4)$$

$$\tau^R \simeq \gamma^R \sim \chi^{-2/3}. \quad (5.5)$$

These results clearly show that as χ increases the most robust states become increasingly amplitude-squeezed. From Eq. (5.1) the scaling law for the rotation angle of the squeezed state is

$$\theta^R \sim \chi^{-1}. \quad (5.6)$$

These scalings with χ can be understood by considering the causes of the decay in the survival probability from the equations (3.16)–(3.20).

A typical highly amplitude-squeezed state member of the most robust ensemble has a mean amplitude-quadrature fluctuation \bar{x} of order unity. From Eq. (3.17), the mean y -quadrature will therefore change in a time $t \ll 1$ by an amount of order χt . This will result in the significant decay of the survival probability if the change χt is of order the standard deviation $\alpha^{1/2}$ of the y -quadrature for that squeezed state. In other words, if $t = \tau$ where

$$\tau \sim \alpha^{1/2} \chi^{-1}. \quad (5.7)$$

The reduction in the overlap due to the motion of the mean phase of the states is plain for the initial states with $\bar{x} = \pm 1$ in Fig. 1(c).

The survival probability will also be affected by an increase in the phase quadrature variance μ_{02} . From Eq. (3.20), the dominant terms for short times are $\mu_{20}(t) - \alpha = -2\chi\beta t + \chi^2\gamma t^2$. Evidently a positive value of the initial x - y covariance β can, at some time t , cancel the increase in the phase variance caused by the nonzero initial amplitude variance γ . This effect will maximize the survival probability if the cancellation occurs at a time of order the survival time τ . This gives the second condition

$$\tau \sim \gamma^{-1} \beta \chi^{-1}. \quad (5.8)$$

This effect is most easily seen for the $\bar{x} = 0$ initial state in Fig. 1(c), where the phase variance at the survival time is little changed from its initial value whereas the phase variance a short time later is significantly changed.

Lastly, we consider the effect of motion and diffusion in the x direction. From Eq. (3.18), the amplitude-quadrature variance increases at a rate of order unity. It will cause a drop in the survival probability once the increase is comparable to the initial amplitude variance $\gamma \sim \alpha^{-1}$, which is at $\tau \sim \gamma$. From Eq. (3.16) the mean amplitude \bar{x} decays to 0 at rate unity, but this will only cause a significant drop in $S(\tau)$ for $\tau \sim \gamma^{-1/2}$, which is much longer. Thus the third condition is just

$$\tau \sim \gamma \sim \alpha^{-1}. \quad (5.9)$$

Once again, the $\bar{x} = 0$ initial state in Fig. 1(c) shows that there is indeed a significant increase in the amplitude variance at t equal to the survival time.

The maximum survival time will clearly be when the survival times from the effects above which cause decay of the survival probability are comparable. The unique solutions to the three analytical scaling relations (5.7)–(5.9) are the scaling laws found numerically and given in equations (5.2)–(5.5) above.

Not only does τ^R scale in the same way as γ^R , it actually asymptotes to γ^R for large χ . This is a consequence of our choice $\Lambda = 1/2$, as will be shown later. In any case, the ensemble-averaged survival time clearly decreases with χ , so that the nonlinearity causes a loss of robustness in the system even under a maximally robust unraveling. However, this loss of robustness is much worse for other ensembles. For example, the coherent state ensemble $E^{|\alpha\rangle}$ has a survival time which varies as

$$\tau^{|\alpha\rangle} \sim \chi^{-1}, \quad (5.10)$$

as shown by the dash-dot-dot curve in Fig. 3. Thus for large χ the description of the laser steady state in terms of the highly amplitude-squeezed states of the most robust ensemble is much more useful than the conventional coherent state description.

The scaling in Eq. (5.10) can be easily derived from Eq. (3.20). Even more simply, it can in fact be derived from the asymptotic analytical formula in Eq. (2.28) for the survival probability for a master equation with a large reversible term. With P a coherent state with $\bar{x} = 0$ and $\mathcal{L}_{\text{rev}} = \mathcal{H}[-i(\chi/4)x^2]$ we find for the solution $S(\tau) = 1/2$,

$$\tau = \sqrt{8}\chi^{-1}. \quad (5.11)$$

Even the coefficient here is a reasonable approximation, as Fig. 3 shows.

3. The Physical Realizability Constraint

Recall that the most robust ensemble $E^{\mathcal{R}}$ is constrained to be physically realizable through the maximally robust unraveling \mathcal{R} . As explained in Sec. IV A 2, this constraint is applied through a nonlinear inequality to be satisfied by the moments γ, β of the members of the ensemble. If we were to ignore these constraints when maximizing τ , we would find the most robust ensemble of the form of Eq. (4.25), unconstrained by having to be physically realizable by an unraveling \mathcal{U} . Such an “unconstrained” ensemble is still constrained first to be equivalent to the stationary state matrix and second to consist of Gaussian pure states, all with the same second-order moments, and with Gaussian-distributed first order moments. The second constraint is not very natural (since we are no longer making any reference to continuous Markovian unravelings). In any case, we will call such an ensemble an unconstrained Gaussian ensemble.

These considerations suggests the obvious question: is the most robust ensemble (as previously defined) different from the most robust unconstrained Gaussian ensemble? That is, are the constraints of physical realizability active in determining the most robust ensemble? The answer depends on the value of χ . Fig. 4 shows the parameters for the most robust unconstrained Gaussian ensemble. For $\chi \gtrsim 7.7$ (where a discontinuity occurs in all of the state parameters) the curves are identical to those of Fig. 3. That is, the constraints of physical realizability are not active. However, for χ less than this value but $\gtrsim 2.7$ the constraints are active and the most robust ensemble is distinct from the most robust unconstrained Gaussian ensemble.

The discontinuities in Figs. 3 and 4, and the unevenness of Fig. 3 for moderate values of χ deserves closer examination. In particular, one can see that in Fig. 3 the solution is on the upper bound of the constraint $\gamma \leq 1$ for $\chi < 5.3$. In Fig. 5 we have plotted the contours of the survival time τ as a function of the state parameters γ and β for different values of χ . Fig. 5(a) verifies that the maximum in τ lies above $\gamma = 1$ for $\chi = 4$.

We have also indicated in Fig. 5 shaded regions representing states which are not physically realizable through monitoring the environment as discussed in Sec. IV.

There is some latitude in the way we choose to monitor the environment, which corresponds in our analysis to the allowed values of the correlation coefficients $u_{ij} = r_{ij} + ih_{ij}$ in Eq. (4.9). The information gained from a particular choice u_{ij} will eventually reduce the laser mode to a pure state represented by the solution α, γ, β of Eqs. (4.20)–(4.22). The case of an optical cavity with one output was discussed in Sec. II B 3. The complicated dynamics of the atom laser mean that some states are not accessible even if all possible u_{ij} are considered.

Given that coherent states are more readily produced experimentally than squeezed states, it may appear odd that the coherent state ($\gamma = 1, \beta = 0$) is not physically realizable for the atom laser with large χ . The reason for this is as follows. The only way the laser mode can be reduced to a coherent state is if the state reduction induced by the monitoring counteracts sufficiently the shearing induced by the nonlinearity represented by χ . To find the values of χ for which this is possible we substitute $\alpha = 1, \gamma = 1, \beta = 0$ and $\nu = 0$ into Eqs. (4.20)–(4.22) and obtain

$$-1 = \frac{1}{2}r_{11} - \frac{1}{2}r_{22} + h_{12}, \quad (5.12)$$

$$-\chi = -\frac{1}{2}h_{11} + \frac{1}{2}h_{22} + r_{12}. \quad (5.13)$$

These equations have a solution satisfying $r_{11}^2 + h_{11}^2 \leq 1$, $r_{12}^2 + h_{12}^2 \leq 1$, and $r_{22}^2 + h_{22}^2 \leq 1$, only for $\chi \leq \sqrt{3}$. This implies that coherent states cannot be realized by monitoring for larger values of χ . As the nonlinearity increases the region representing non-realizable states grows outwards from the coherent state point ($\gamma = 1, \beta = 0$), as illustrated in Fig. 5(a) and Fig. 5(b) for increasing χ values.

Returning to Fig. 3, the “kink” in the α and β curves at $\chi \approx 2.7$ is the point where the non-realizable region has grown so that its boundary reaches the point of maximum τ on the $\gamma = 1$ line. The maximally robust ensemble remains on the intersection of the boundary of the non-realizable region and the line $\gamma = 1$ until $\chi \approx 5.3$ where the maximum of τ occurs on the boundary at $\gamma \approx 0.71$. For χ increasing up to about 7.4 the maximally robust state continues to lie on the boundary of the non-realizable region, and for $\chi \gtrsim 7.4$ the maximally robust state moves away from the non-realizable region as shown in Fig. 5(b). At $\chi \approx 7.7$ the local maximum of τ outside the non-realizable region becomes the global maximum and the unconstrained ensemble shown in Fig. 4 jumps to become identical with the constrained ensemble.

B. Varying ν

Before considering the effect of varying ν as we have done above for χ , we first present the effect of choosing a moderate but non-zero value of ν on the results we have already obtained. The new version of Fig. 4 with $\nu = 2.5$ is shown as Fig. 6. This value of ν implies excess phase diffusion comparable to the intrinsic phase diffusion of an

ideal laser. The effect of this excess phase diffusion is to wash out the complicated structures for moderate values of χ , and to leave the large χ behaviour unchanged. Furthermore, it can be shown that the constraints of physical realizability play no role in determining these most robust ensembles. However, this is no longer true for $\nu = 2.5$ if the value of Λ is changed, as will be discussed later.

Figure 7 is an overview of the most robust ensemble for $\chi = 0$ and for ν ranging from 1 to 1000. The behaviour is very simple. For $\nu \lesssim 2.5$ the most robust states are coherent states. As ν increases they become increasingly squeezed states. For all values of ν we have $\beta = 0$ (which is therefore not plotted), indicating that the most robust states are purely amplitude-squeezed. The scaling laws derived from this plot are

$$\alpha^R \sim \nu^{1/2}, \quad (5.14)$$

$$\gamma^R \sim \nu^{-1/2}, \quad (5.15)$$

$$\tau^R \simeq \gamma^R \sim \nu^{-1/2}. \quad (5.16)$$

These scaling can again be deduced by arguments similar to those in Sec. V A 2. Unlike the nonlinear χ term, phase diffusion does not cause motion of the mean position of a typical squeezed state. Rather, from Eq. (3.20), it simply causes the phase-quadrature variance to increase linearly as $\nu\tau$. The survival probability will drop significantly in this time if $\nu\tau$ is comparable to the original phase variance, α . From the increase in the amplitude variance we get $\tau \sim \gamma^{-1} \sim \alpha$ as in Sec. V A 2. The maximum survival time occurs when these two times are comparable, giving $\tau^R \sim \nu^{-1/2}$ and $\alpha^R \sim \nu^{1/2}$, as found numerically.

The survival time decreases with increasing ν , and, once again, it asymptotes to γ^R for large ν . For comparison we also plot the survival time $\tau^{|\alpha\rangle}$ for a coherent state ensemble. This scales as

$$\tau^{|\alpha\rangle} \sim \nu^{-1}, \quad (5.17)$$

so that for large ν the most robust ensemble is much more robust than the coherent state ensemble. This scaling can be derived from the short time asymptotic analytic expression in Eq. (2.26). Since the excess phase diffusion dominates the evolution for ν large we have approximately

$$S(\tau) \simeq 1 + \nu t \text{Tr}\{PD[x/2]P\}. \quad (5.18)$$

Again, this expression only applies for a single state or an ensemble such as the coherent state ensemble where all members are effectively identical.

It can be shown that the most robust ensemble for $\chi = 0$ is identical to the unconstrained Gaussian ensemble for all values of ν . Also, for $\chi = 0$, the coherent state ensemble is a physically realizable ensemble for all values of ν . For these reasons we have not presented plots analogous to those in Figs. 4 and 5.

C. Varying Λ

The final parameter we wish to consider varying is Λ , which defines the survival time τ by the equation $S(\tau) = \Lambda$. All of the results presented so far were for $\Lambda = 0.5$. In Fig. 8 we show the parameters α^R and τ^R for the most robust ensemble as a function of χ for $\nu = 200$ and for four values of Λ . This value of ν was chosen so that the maximally robust state solutions would not feel the constraints of physical realizability. For large χ the slope of the curves are independent of Λ . Thus the scaling laws established in Sec. V A are independent of Λ . As Λ decreases, the survival time τ^R increases, because it takes longer for the survival probability to decay to that level.

Decreasing Λ also causes the phase variance α^R to increase, indicating that the most robust states are more highly squeezed. This is not unexpected, since the difference between the coherent state ensemble and the most robust ensemble is expected to be greater at longer times by the argument in Sec. V A 1. However, the relative increase in α^R is far less than the relative increase in τ^R . In other words, the most robust ensemble is only weakly dependent on Λ . Interestingly, because $\gamma^R \sim 1/\alpha^R$, γ^R decreases as Λ decreases, while τ^R increases. Thus the asymptotic result $\gamma^R \simeq \tau^R$ can only be true at one value of Λ , namely $\Lambda = 1/2$.

Figure 9 presents the same information as Fig. 8 but for $\chi = 0$ and varying ν and Λ . Once again the scaling laws established in Sec. V B are found to be independent of Λ , and in this case the different values for α^R appear to asymptote. In this case, the value for ν above which the coherent state ensemble ceases to be the most robust ensemble increases for decreasing Λ . Above these values of ν the amplitude-squeezing in the most robust ensemble is always decreased as Λ is decreased. However, the difference is small (and may vanish as $\nu \rightarrow \infty$), so that the equation $\tau^R \simeq \gamma^R$ is again valid only for $\Lambda = 1/2$. The sum of these results justifies our use of the single value $\Lambda = 1/2$ for most of this work.

VI. DISCUSSION

A. Summary

The atom laser, even in the single-mode approximation, is an open quantum system with rich dynamics. In this paper we have explored a new way of characterizing those dynamics: finding the maximally robust unraveling [21]. This yields a maximally robust ensemble E^R of pure states P^R which comprise the *physically realizable* states which survive the best. By “surviving”, we mean remaining unaffected by the system dynamics. This ensemble is, we have argued, the most natural representation of the stationary state matrix ρ_{ss} of the laser; if one wished

to regard the laser as being “really” in a pure state, then the states to choose are the members of this ensemble. Although it is a time-independent ensemble, it is drastically affected by alterations in the dynamics of the atom laser, even though those alterations do not change the stationary state matrix.

We considered a simple model for the atom laser in which ρ_{ss} is a Poissonian mixture of number states of mean μ . Working in the linearized regime, we identified two relevant dynamical parameters which may be varied without altering this stationary state. The first is χ , which is proportional to the strength of self-interaction energy of the atoms in the laser [see Eqs. (3.3) and (3.9)]. The second is ν , which is proportional to the excess phase diffusion of the laser above the standard quantum limit.

For $\chi = 0$ and ν small, the maximally robust ensemble was found to consist of coherent states, with mean boson number μ but with all possible phases. This is the most common representation of the state of the laser, and so is not surprising. In terms of the parameters we used in the paper, the ensemble consisted of Gaussian pure states with phase quadrature variance $\alpha = 1$, amplitude-quadrature variance $\gamma = 1$, and amplitude-phase covariance $\beta = 0$.

As the self-energy χ is increased the most robust states cease to be coherent states. In fact, for any value of χ above $\sqrt{3}$, not only are the coherent states not the most robust state; in addition they are not even physically realizable. That is to say, there is no possible way to monitor the baths to which the laser is coupled which would reduce the state of the laser to a coherent state. This means that the picture of a laser as a mixture of coherent states of unknown phase is *physically meaningless* if $\chi > \sqrt{3}$. We will return to this point later.

For large values of χ the most robust states P^R are very highly amplitude-squeezed states with amplitude-quadrature variance γ^R scaling as $\chi^{-2/3}$ and phase quadrature variance α^R scaling as $\chi^{2/3}$. The same effect occurs for large values of ν , with scalings of $\nu^{-1/2}$ and $\nu^{1/2}$ respectively.

As noted above, our analysis was based on a linearized approximation for the laser dynamics. This is only valid if the states under consideration have a well-defined coherent amplitude. As χ or ν are increased indefinitely and the most robust states become more amplitude-squeezed, this approximation will clearly break down. Specifically, it will break down when the phase variance predicted by the linearized analysis is of order unity; that is, when the phase quadrature variance α^R is of order the mean boson number μ . From the above scalings, for the linearization to remain valid we require

$$\chi \ll \mu^{3/2}, \quad (6.1)$$

$$\nu \ll \mu^2. \quad (6.2)$$

Although we cannot say with confidence what the most robust states are when the linearization breaks down, we do know that they must be states without a well-defined

coherent amplitude (because that is why the linearization breaks down). Therefore the conditions in Eqs. (6.1) and (6.2) also represent the conditions for the most robust states to be states with well-defined coherent amplitudes. In other words, if and only if these conditions are satisfied, the most natural description of the atom laser is in terms of states with a mean field.

B. Interpretation

We can now finally state the most important result of this paper. The conditions (6.1) and (6.2) are identical to the previously derived conditions (3.27) and (3.28) for the output of the device to be coherent. Here we mean coherent in the sense that the output is quantum degenerate, with many bosons being emitted per coherence time. Without this condition the device could not be considered a laser at all, as its output would consist of independent atoms rather than a matter wave.

The significance of this result is that there is a perfect correspondence between the pure states the laser is “really” in and the coherence of its output. If the most robust states have a well-defined coherent amplitude, like coherent states, then the output is coherent. If the most robust states do not have a well-defined coherent amplitude, like number states, then the output is not coherent. This profound result establishes beyond doubt the usefulness of maximally robust unravelings as an investigational tool for open quantum systems.

It must be emphasized that the link between the presence or absence of a mean field inside the laser, and the presence or absence of quantum coherence in the laser output, is not due to any simple relationship of definitions. Finding the maximally robust ensemble is, as the diligent reader will appreciate, a very involved process completely different from calculating the first-order coherence function. In particular, the average survival time for the members of the most robust ensemble has in general no relationship with the coherence time.

It is also worth pointing out that the relationship we have established between robust mean-field states and quantum degeneracy would not have been found had we used purity rather than survival probability as the basis of our definition for the maximally robust ensemble. Although there are no great differences between the two definitions as one varies ν , there is a great difference as one varies χ . This is to be expected from the analysis in Sec. II C 2, as χ represents a self-energy term which is Hamiltonian, whereas ν represents irreversible phase diffusion.

To prove this point we have calculated the ensemble which maximizes the time it takes for the average purity of the member states [as defined in Eq. (2.20)] to drop to $1/2$ under the master equation evolution. We plot the parameters for this ensemble as a function of χ in Fig. 10. For comparison we also plot the phase quadra-

ture variance α^R and the survival time τ^R of the most robust ensemble as previously defined, in terms of survival probability. The ensemble parameters when we use purity obey scaling laws for large χ , but they are different from those scaling laws obtained when using the survival probability (Sec. V A 2):

$$\alpha \sim \chi^{1/2}, \quad (6.3)$$

$$\gamma \sim \chi^{-1/2} \quad (6.4)$$

$$\beta \sim 1, \quad (6.5)$$

$$\tau \sim \chi^{-1/2}. \quad (6.6)$$

As expected from Sec. II C 2, the purity half-life is much longer than the survival time for large χ .

The condition for the best purity preserving states to have a well-defined coherent amplitude is $\alpha \ll \mu$ which from the above scalings gives

$$\chi \ll \mu^2. \quad (6.7)$$

This implies that there is a range of interaction strengths $\mu^{3/2} \lesssim \chi \ll \mu^2$ for which the purity analysis delivers a description of the laser in terms of states with a mean field even though the laser output is no longer coherent in the sense defined above. It is conceivable that there is some more subtle property of the laser output which is correlated with the nature of the best purity-preserving states, but we have not been able to establish this.

C. Experimental Implications

In the Introduction we motivated our exploration of the atom laser by asking the question, is an atom laser “really” a mixture of number states, or “really” a mixture of coherent states? We can now state the answer: it depends. If the device is a true laser, with a quantum degenerate output, then it is most natural to regard it as being in a state with a well-defined coherent amplitude like a coherent state, but, more generally, with amplitude-squeezing. In the opposite limit, where the device emits independent atoms, it is most natural to regard it as being in a state without a well-defined coherent amplitude, like a number state.

These answers suggest another question, namely, what is the situation for experimental atom lasers? As discussed in the introduction, a number of experimental groups have realized Bose-Einstein condensates with output coupling [17–20]. A true atom laser would have to incorporate a mechanism for replenishing the condensate so that the output coupling could continue indefinitely. Nevertheless we can take these experiments as a possible indication for the parameter regime in which an atom laser may work. The figures below are derived by setting the bare linewidth κ of the laser equal to the reciprocal of the lifetime of the condensates in the experiment, and the mean atom number μ equal to the initial occupation

number of the condensate. The excess phase diffusion ν we have ignored, and we have calculated χ using Eq. (3.3) and Eq. (3.9).

Most current experiments work in the regime where the ratio of the kinetic energy to the interaction energy is very small [38]:

$$\left(\frac{\hbar}{64\pi^2 m \omega \mu^2 a_s^2} \right)^{2/5} \ll 1. \quad (6.8)$$

Here m is the atomic mass, ω is the mean trap frequency, and a_s is the scattering length as in Eq. (3.3). In this regime the Thomas-Fermi approximation can be made, allowing us to evaluate χ analytically as

$$\chi = \frac{4}{7\kappa} \left(\frac{225\mu^2 m \omega^6 a_s^2}{\hbar} \right)^{1/5}. \quad (6.9)$$

For the first “pulsed atom laser” experiment with Sodium [17] the above formula gives $\chi \approx 1100$. For the more recent quasicontinuous output coupling [19], also with Sodium, we get $\chi \approx 50$. Finally, the parameters for the continuous output coupling of a Rubidium condensate [20] yields $\chi \approx 1400$.

All of these values are in the large χ regime which we have concentrated on in this paper. Thus if these experiments could be run with the same output coupling but with continuous replenishment of the condensate, the most robust ensemble would comprise highly amplitude-squeezed states rather than coherent states. For $\chi = 1000$ the standard deviation of the amplitude-quadrature of these states would be of order 0.1, compared to 1 for coherent states. Moreover, since $\chi > \sqrt{3}$, there is no physical way to realize the ensemble comprising coherent states. In summary an atom laser should not be thought of as being in a coherent state.

Despite the banishing of the coherent state description, truly continuous versions of the experiments analyzed above would produce a coherent (quantum degenerate) output and the most robust states would have a well-defined coherent amplitude, as long as the excess phase diffusion were not too large. That is because the calculated values of χ are always much less than $\mu^{3/2}$, so that Eq. (6.1) above is satisfied. Interestingly, we can recast this condition in terms of the output flux $I = \kappa\mu$ (atoms per unit time) as

$$I \gg 1.61 \omega \left(\frac{a_s^4 \omega m^2 \kappa}{\hbar^2} \right)^{1/11} \quad (6.10)$$

This inequality depends very weakly on the dimensionless quantity in brackets because of the 11th root. For the above three experiments this 11th root averages to 0.16, and ranges only from 0.13 to 0.21. Hence we can state the coherence condition for an atom laser in terms essentially independent of the species and decay time as $I \gg 0.26\omega$ or

$$I \gg T^{-1}. \quad (6.11)$$

That is, there should be many atoms emitted into the laser beam per oscillation period $T = 2\pi/\omega$ of the trap. This is such a simple rule of thumb that it should be useful, but it must be remembered that there is no direct physical connection between the flux and the trap frequency. This result is simply a numerical coincidence arising from the various physical parameters for atomic Bose-Einstein condensation in typical traps.

D. Future Work

There are at least three future directions for this work.

First, the insights into the atom laser which the maximally robust unravelings analysis offers suggests that this technique could be applied fruitfully to other open quantum systems. Examples include other models for Bose-Einstein condensates in equilibrium with a reservoir [39], fluorescent atoms and other quantum optical systems [26,27]. These are systems with nontrivial dynamics which could be more fully appreciated by determining the maximally robust unraveling.

Second, the difference between the analyses based on survival probability and purity deserves further investigation. As we showed, the purity analysis gives a description of the laser mode in terms of states with a well-defined coherent amplitude for high values of χ where the survival analysis does not, and where the output is not coherent in the conventional sense. This suggests [40], in particular, that the properties of the output under these circumstances should be studied more closely.

Finally, there are other approaches to quantifying the robustness of unravelings apart from the survival probability and the purity. For example, one could measure how quickly the unraveling purifies the state, or how sensitive the purity is to imperfections in the unravelings. These ideas could be best investigated in systems somewhat simpler than the atom laser we have considered here. This would give an indication for the robustness of the idea of robustness; that is, how sensitive the maximally robust unraveling is to the definition of robustness used, and which definitions agree.

To conclude, the clear and simple interpretation for the results we have obtained here for the atom laser vindicates our conviction [21] that maximally robust unravelings have a role as a tool for understanding the dynamics of open quantum systems, and that this will be an increasing role in the future.

- [1] K. Mølmer, Phys. Rev. A **55**, 3195 (1996).
- [2] J. Gea-Banacloche, Phys. Rev. A **58**, 4244 (1998); K. Mølmer, *ibid.*, 4247 (1998).
- [3] H.M. Wiseman, Phys. Rev. A **56**, 2068 (1997).

- [4] J. Gea-Banacloche, in: *New Frontiers in Quantum Electrodynamics and Quantum Optics*, A.O. Barut, ed., Plenum, New York (1990).
- [5] H.M. Wiseman, Phys. Rev. A **47**, 5180 (1993).
- [6] J. Gea-Banacloche, Found. Phys. **28**, 531 (1998).
- [7] M. Sargent, M.O. Scully, and W.E. Lamb, *Laser Physics* (Addison-Wesley, Reading Mass., 1974)
- [8] S.M. Barnett, K. Burnett and J.A. Vaccaro, J. Res. Natl. Inst. Stand. Technol. **101**, 593 (1996).
- [9] B. Schumacher, Phys. Rev. A **51**, 2738 (1995).
- [10] H.M. Wiseman and M.J. Collett, Phys. Lett. A **202**, 246 (1995).
- [11] R.J.C. Spreeuw, T. Pfau, U. Janicke, and M. Wilkens, Europhys. Lett. **32**, 469 (1995).
- [12] M. Olshanii, Y. Castin, and J. Dalibard, in *Proc. XII Conference on Lasers Spectroscopy*, edited by M. Inguscio, M. Allegrini and A. Sasso (World Scientific, 1995).
- [13] M. Holland *et al.*, Phys. Rev. A **54**, R1757 (1996).
- [14] M.H. Anderson *et al.*, Science **269**, 198 (1995).
- [15] C.C Bradley, C.A. Sackett, J.J. Tollett, and R.G. Hulet, Phys. Rev. Lett. **75**, 1687 (1995).
- [16] K.B. Davis *et al.*, Phys. Rev. Lett. **75**, 3969 (1995).
- [17] M.-O. Mewes, M. R. Andrews, D. M. Kurn, D. S. Durfee, C. G. Townsend, and W. Ketterle, Phys. Rev. Lett. **78**, 582 (1997).
- [18] B.P. Anderson, M.A. Kasevich, Science **282**, 1686 (1998).
- [19] E.W. Hagley, L. Deng, M. Kozuma, J. Wen, K. Helmerson, S.L. Rolston, W.D. Phillips, Science **283**, 1706 (1999);
- [20] I. Bloch, T.W. Hänsch, and T. Esslinger Phys. Rev. Lett. **82**, 3008 (1999).
- [21] H.M. Wiseman and J.A. Vaccaro, Phys. Lett. A **250**, 241 (1998).
- [22] W.H. Zurek, Prog. Theor. Phys. **89**, 281 (1993).
- [23] W.H. Zurek, S. Habib, and J.P. Paz, Phys. Rev. Lett **70**, 1187 (1993).
- [24] M.R. Gallis, Phys. Rev. A **53**, 655 (1996).
- [25] Gh.-S. Paraoanu and H. Scutaru Phys. Lett. A **238**, 219 (1998).
- [26] H.J. Carmichael, *An Open Systems Approach to Quantum Optics* (Springer-Verlag, Berlin, 1993).
- [27] C.W. Gardiner, *Quantum Noise* (Springer, Berlin, 1991).
- [28] G. Lindblad, Commun. math. Phys. **48**, 199 (1976).
- [29] J. Dalibard, Y. Castin and K. Mølmer, Phys. Rev. Lett. **68**, 580 (1992).
- [30] C.W. Gardiner, A.S. Parkins, and P. Zoller, Phys. Rev. A **46**, 4363 (1992).
- [31] H.M. Wiseman and G.J. Milburn, Phys. Rev. A **47**, 1652 (1993).
- [32] Quant. Semiclass. Opt. **8** (1) (1996), special issue on “Stochastic quantum optics”, edited by H.J. Carmichael.
- [33] C.W. Gardiner, *Handbook of Stochastic Methods* (Springer, Berlin, 1985).
- [34] J. Cresser, private communication.
- [35] M. Rigo and N. Gisin, p. 255 of Ref. [32] (1996).
- [36] H.M. Wiseman, p. 205 of Ref. [32] (1996).
- [37] In Ref. [8] we used the same overlap as in Eq. (2.17) as a measure of robustness which, following Ref. [9], we referred to as fidelity. However, we feel that the term *survival probability* is more appropriate since it embodies

the notion of the state P_i^U to survive over time t whereas *fidelity* embodies the faithful reproduction of a state.

[38] G. Baym and C.J. Pethick, Phys. Rev. Lett. **76**, 6 (1996).
 [39] J. Anglin, Phys. Rev. Lett. **79**, 6 (1997).
 [40] The criteria we used for determining the coherence of the output is based on the first-order correlation function. This measure involves an ensemble average and so is insensitive to the different frequencies evident in Fig. 1c for different members of an ensemble. A different measure might reveal subtle coherence properties under these circumstances.

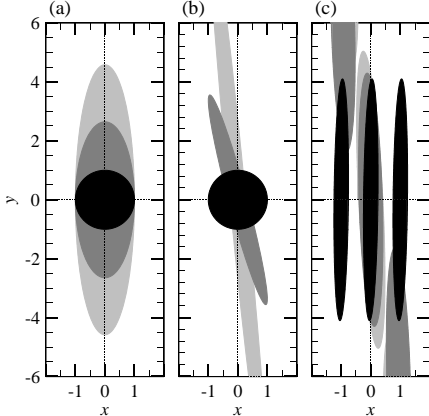


FIG. 1. The evolution of (initially pure) Gaussian quantum states under the master equation (3.8) for three different cases. The states are represented by the one standard-deviation ellipse of the Wigner function. In each case we choose the initial mean location of the state in phase space to be $\bar{x} = \bar{y} = 0$, except for the last where we also have $\bar{x} = \pm 1$. For all three cases the excess phase diffusion is $\nu = 0$. For case (a) we have $\chi = 0$ and an initially coherent state (which forms the most robust ensemble in this case). For case (b) we have $\chi = 100$ and again an initially coherent state. For case (c) we have $\chi = 100$ but the initial states are members of the most robust ensemble for this case. In all cases the black ellipses are for $t = 0$, the dark grey ellipses for $t = \tau$ (the appropriate ensemble-averaged survival time), and the light grey ellipses for a still later time. For details of these times see the main text.

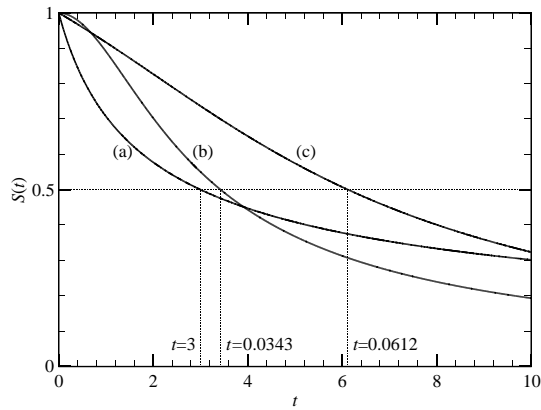


FIG. 2. The decay of the ensemble-averaged survival probability in time for the three cases represented in Fig. 1. The three cases are: (a) coherent state ensemble with $\chi = 0, \nu = 0$; (b) coherent state ensemble with $\chi = 100, \nu = 0$; (c) most robust ensemble with $\chi = 100, \nu = 0$. The horizontal axis measures time t . For case (a) it is scaled in units of the bare lifetime of the laser mode, and for cases (b) and (c) it is scaled in units 100 times smaller. That is, the survival probabilities actually drop much more quickly for cases (b) and (c).

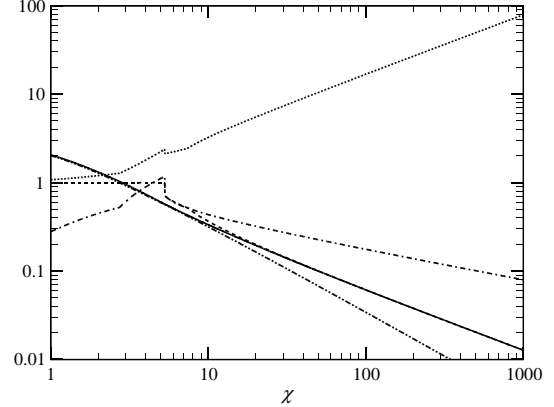


FIG. 3. The parameters for the ensemble arising from the maximally robust unraveling \mathcal{R} as a function of χ with $\nu = 0$. These parameters are the phase quadrature variance α^R (dotted line), the amplitude-quadrature variance γ^R (dashed line) and the covariance β^R (dash-dot line) for the members of this ensemble. We also plot the survival time τ^R (solid line) of this ensemble and, for comparison, the survival time $\tau^{|α\rangle}$ (dash-dot-dot line) of a coherent state ensemble. Both of these times are in units of the bare lifetime of the laser mode.

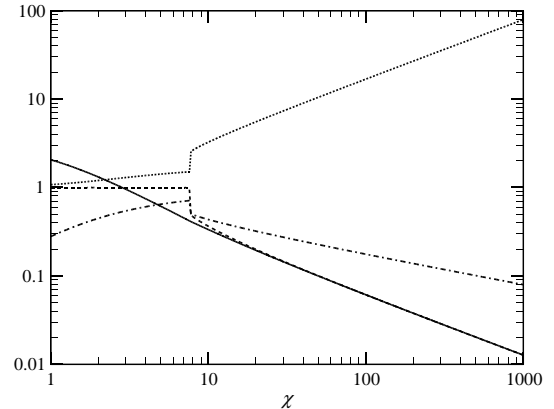


FIG. 4. The parameters for the most robust unconstrained Gaussian ensemble as a function of χ with $\nu = 0$. Here unconstrained means that these ensembles do not have to be physically realizable. As in Fig. 3 we plot α (dotted line), γ (dashed line), β (dash-dot line) and τ (solid line) (in units of the bare lifetime of the laser mode).

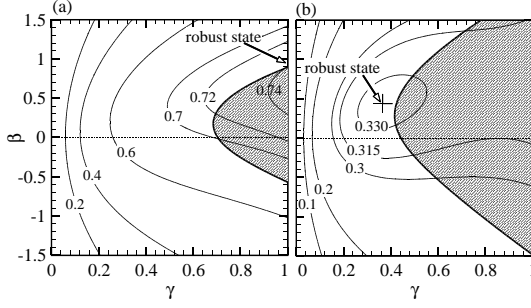


FIG. 5. Contour plots of the survival time τ as a function of γ and β . In (a) $\nu = 0$ and $\chi = 4$ and in (b) $\nu = 0$ and $\chi = 10$. In each plot the light curves represent contours of τ (in units of the bare lifetime of the laser mode) and the shaded region represents states which are not physically realizable using the monitoring scheme discussed in the text.

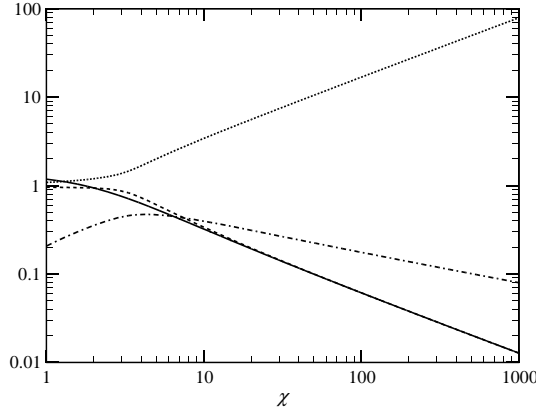


FIG. 6. The parameters for the ensemble arising from the maximally robust unraveling \mathcal{R} as a function of χ with $\nu = 2.5$. As in Fig. 3 we plot $\alpha^{\mathcal{R}}$ (dotted line), $\gamma^{\mathcal{R}}$ (dashed line), $\beta^{\mathcal{R}}$ (dash-dot line) and the survival time $\tau^{\mathcal{R}}$ (solid line) (in units of the bare lifetime of the laser mode).

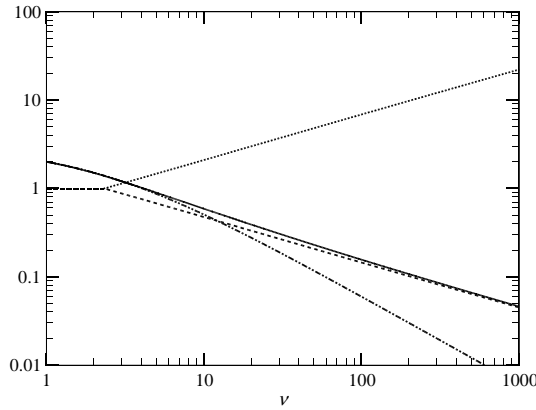


FIG. 7. The parameters for the ensemble arising from the maximally robust unraveling \mathcal{R} as a function of ν with $\chi = 0$. As in Fig. 3 we plot $\alpha^{\mathcal{R}}$ (dotted line), $\gamma^{\mathcal{R}}$ (dashed line), and the survival time $\tau^{\mathcal{R}}$ (solid line). We do not plot $\beta^{\mathcal{R}}$ because it is identically zero. For comparison we also plot the survival time $\tau^{|\alpha\rangle}$ (dash-dot-dotted) of a coherent state ensemble. Both of these times are in units of the bare lifetime of the laser mode.

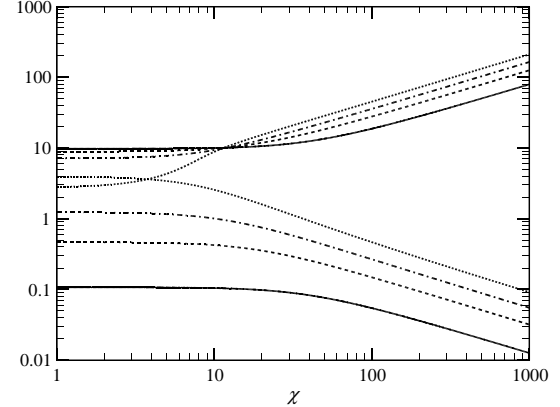


FIG. 8. The parameters for the ensemble arising from the maximally robust unraveling \mathcal{R} as a function of χ with $\nu = 200$ and for various Λ . The rising lines are $\alpha^{\mathcal{R}}$ and the falling lines are $\tau^{\mathcal{R}}$ (in units of the bare lifetime of the laser mode). The values of Λ are 0.5 (solid line), 0.2 (dashed line), 0.1 (dash-dot line), and 0.05 (dotted line).

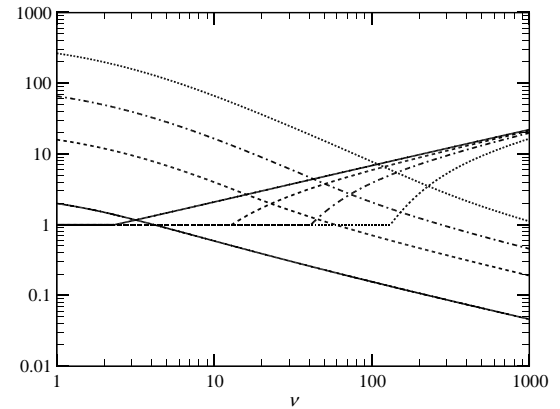


FIG. 9. The parameters for the ensemble arising from the maximally robust unraveling \mathcal{R} as a function of ν with $\chi = 0$ and for various Λ . The rising lines are $\alpha^{\mathcal{R}}$ and the falling lines are $\tau^{\mathcal{R}}$ (in units of the bare lifetime of the laser mode). The values of Λ are 0.5 (solid line), 0.2 (dashed line), 0.1 (dash-dot line), and 0.05 (dotted line).

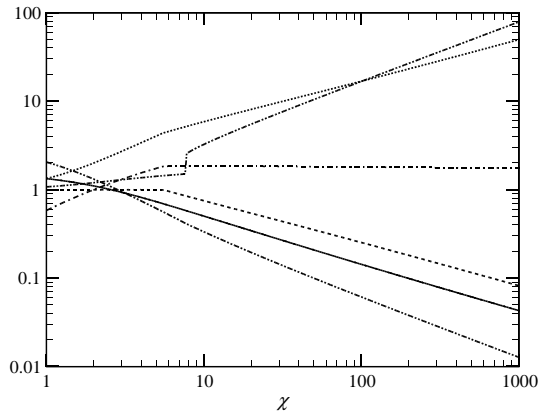


FIG. 10. Parameters for the maximally robust ensemble for $\nu = 0$ as a function of χ as in Fig. 4 but using purity as a measure of robustness. As in previous figures we plot α (dotted line), γ (dashed line), β (dash-dot line) and τ (solid line). Also shown for comparison are the α (rising) and τ (falling) curves from Fig. 4 as dash-dot-dotted curves. Both times are in units of the bare lifetime of the laser mode.